

FUNCTIONALIZED MEMBRANES FOR MEMBRANE CHROMATOGRAPHY

by

JAYRAJ SHETHJI

STEPHEN M.C. RITCHIE, Ph.D., COMMITTEE CHAIR

CHRISTOPHER S. BRAZEL, Ph.D.

DAVID E. NIKLES, Ph.D.

A THESIS

Submitted in partial fulfillment of the requirements
for the degree of Master of Science in the
Department of Chemical and Biological
Engineering in the Graduate School
of The University of Alabama

TUSCALOOSA, ALABAMA

2011

Copyright Jayraj Shethji 2011
ALL RIGHTS RESERVED

ABSTRACT

The focus of this thesis is synthesis and quantification of homopolymer and block copolymer grafts and understanding controlled polymer growth. The homopolymer and block copolymer grafts were synthesized through sequential cationic polymerization of styrene and substituted styrene monomers chloromethylstyrene (CMS) and 4-ethoxystyrene (ES) in the pores of microfiltration polyethersulfone (PES) membrane. Polymer growth aspects like kinetics of reaction, amount of monomer reacted, ion-exchange capacity (IEC), and graft length were studied with respect to initiator contact time and monomer feed concentration.

Functionalization of the microfiltration membrane was achieved by a two step procedure. The first step was to introduce sulfonic acid initiator sites by mild sulfonation with 0.5N H₂SO₄. This was followed by cycling through each type of monomer solution (styrene and substituted styrenes). Successful introduction of homopolymer and block copolymer grafts was confirmed by material balances on the monomer/toluene permeate solutions. Analytical techniques used for quantification of polymer grafting include UV-Visible spectroscopy, gas chromatography and atomic absorption. The functionalized membrane showed a steep decrease in membrane permeability compared to the raw membrane indicating the presence of polymeric chains in the membrane flow path. Functionalized membranes prepared by this method have as many as 125 repeat units per chain. Given the initiator concentration, this equates to an IEC of 4.9 meq/g, indicating high dynamic and equilibrium binding capacity.

Pseudo-first-order kinetic expression correlated well with the experimental data for each monomer reacted. At lower initiator surface density, graft length and IEC were impacted by both monomer feed concentration and initiator contact time. However, for higher initiator surface density, monomer feed concentration parameter dominates.

Block copolymer formation is the first step to synthesizing an analog of the phenylalanine/tyrosine dipeptide structure in protein A, which is shown in literature for selective adsorption of immunoglobulin G (IgG). This work will lead to further development of functionalized membranes as membrane adsorbers for high throughput production of monoclonal antibodies for new cancer therapies. In addition, it will lead to discoveries in sequential polymerization to generate customized structures and design of synthetic affinity ligands.

ACKNOWLEDGEMENTS

The author wishes to express his solemn gratitude to Dr. Stephen Ritchie for his support, counseling and patience throughout the period of research. The author would also like to thank him for showing faith in abilities and giving independent responsibilities and various opportunities. It was a great learning value working with him and his editorial help in the preparation of this manuscript is greatly acknowledged. Gratitude is also extended to other members of the supervisory committee, Dr. Christopher S. Brazel and Dr. David E. Nikles, for their supervision and interest in this work.

The author is thankful to the faculty, staff and graduate students of Department of Chemical Engineering for making this research journey an enjoyable experience. The author would also like to thank Soubantika Palchoudhury for her help and support. Help from Ryan Beam and Lukai Yang from membrane research group is also acknowledged. The financial support from the National Science Foundation and Department of Chemical and Biological Engineering is also gratefully acknowledged and appreciated.

Finally, the author expresses gratitude to his parents Kanan Shethji and Kirit Shethji and wife Nikita for their continuous encouragement and support.

CONTENTS

ABSTRACT	ii
ACKNOWLEDGEMENTS	iv
LIST OF TABLES	ix
LIST OF FIGURES	x
1. INTRODUCTION	1
1.1 Technological background.....	1
1.2 Immunoglobulin G (IgG) and Protein A binding chemistry.....	5
1.3 List of research objectives	7
1.4 Approach.....	8
2. BACKGROUND AND THEORY	10
2.1 Introduction.....	10
2.2 Monoclonal antibodies (MAbs)	10
2.2.1 Definition	10
2.2.2 Applications of MAbs.....	11
2.2.3 Purification of MAbs	12
2.3 Affinity chromatography	12
2.3.1 Principle	12
2.3.2 Applications	13
2.3.3 Ligands in affinity chromatography.....	13

2.3.3.1	Affinity ligands for immunoglobulins.....	14
2.3.3.2	Synthetic (Biomimetic) ligands.....	15
2.3.4	Limitations of affinity chromatography.....	18
2.4	Membrane chromatography.....	19
2.4.1	Advantages over affinity chromatography.....	19
2.4.2	Affinity membranes for protein purification.....	21
2.4.3	Challenges for improvement in membrane chromatography.....	23
2.5	Functionalized membranes.....	24
2.5.1	Principle.....	24
2.5.2	Introduction to polymer brushes.....	25
2.5.3	Classification of polymer brushes.....	25
2.5.4	Graft polymerization by chemical techniques.....	27
2.6	Cationic polymerization.....	28
3.	EXPERIMENTAL PROCEDURE.....	32
3.1	Introduction.....	32
3.2	Materials.....	32
3.3	Methods.....	34
3.3.1	Initiator immobilization.....	36
3.3.2	Synthesis of homopolymer brush.....	36
3.3.3	Synthesis of block copolymer brush in the membrane matrix.....	37
3.3.4	Membrane permeability.....	37
3.4	Analysis.....	38
3.4.1	Ion-exchange capacity (IEC).....	38

3.4.2 UV-Visible spectroscopy analysis	40
3.4.3 Gas chromatography analysis	44
4. RESULTS AND DISCUSSION	47
4.1 Introduction.....	47
4.2 Membrane permeability studies.....	47
4.3 Quantification of membrane sulfonation	50
4.4 Synthesis and quantification of homopolymer brushes	51
4.4.1 Styrene and CMS graft quantification by UV-Visible spectroscopy.....	51
4.4.2 4-Ethoxystyrene graft quantification by gas chromatography.....	53
4.4.3 Kinetics of each monomer reacted.....	56
4.5 Kinetics of CMS/ES during formation of block copolymer grafts	60
4.6 Controlled polymer growth.....	60
4.6.1 Introduction.....	60
4.6.2 Influence of monomer concentration	62
4.6.2.1 Kinetics.....	62
4.6.2.2 Graft length.....	64
4.6.3 Influence of initiator reaction time	66
4.6.3.1 Monomer reacted.....	66
4.6.3.2 Graft length.....	66
4.6.3.3 Ion-exchange capacity.....	69
4.6.4 Summary of results from polymer growth experiments	71
4.6.4.1 Ion-exchange capacity	71
4.6.4.2 Graft length	72

5. CONCLUSIONS.....	73
6. FUTURE WORK AND SCOPE.....	75
REFERENCES.....	76

LIST OF TABLES

Table 3-1 Gas chromatograph column parameters.....	45
Table 4-1 Pseudo-first-order model parameters.....	58

LIST OF FIGURES

Figure 1-1 Schematic of (a) PES membrane cross-section; (b) representative polymer graft; and (c) heterogeneous binding site.....	3
Figure 1-2 Phenylalanine-tyrosine dipeptide structure.....	4
Figure 1-3 Schematic representation of an IgG molecule.....	6
Figure 1-4 Experimental approach for functionalization of PES microfiltration membrane.....	9
Figure 2-1 Chemical structure of TG19318.....	17
Figure 2-2 Solute transport in membrane and packed bed (pore diameter 100-200 nm) chromatography.....	20
Figure 2-3 Classification of linear polymer brushes: (a ₁ -a ₄) homopolymer brushes, (b) mixed polymer brush, (c) random copolymer brush, and (d) block copolymer brush.....	26
Figure 2-4 Propagation step for cationic polymerization of styrene.....	29
Figure 2-5 Polystyrene grafts in a membrane pore.....	31
Figure 3-1 Repeat unit structure of polyethersulfone.....	33
Figure 3-2 Schematic of the experimental laboratory setup.....	35
Figure 3-3 Standard calibration curve for IEC analysis by atomic absorption spectroscopy using sodium ion ($\lambda = 589$ nm).....	39
Figure 3-4 UV-spectrum of (a) pure styrene showing characteristic peak at 291 nm, and (b) UV-spectrum of pure CMS showing characteristic peak at 295 nm.....	41

Figure 3-5 UV-spectrum of pure toluene showing characteristic peak at 281 nm.....	42
Figure 3-6 Standard calibration curve for styrene analysis at 291 nm by UV- spectrophotometry.....	43
Figure 3-7 Standard calibration curve for ES analysis by gas chromatography.....	46
Figure 4-1 Polymer growth effect on membrane permeability.....	49
Figure 4-2 UV-VIS spectrum for quantification of (a) styrene disappearance, and (b) CMS disappearance.....	52
Figure 4-3 UV-spectrum of 4-ethoxystyrene and toluene showing characteristic peak at 283 and 281 nm, respectively.....	54
Figure 4-4 Gas chromatogram for quantification of ES disappearance.....	55
Figure 4-5 Kinetics of each monomer reacted. The smooth curves represent the pseudo-first- order equation fit and the data points represent experimental observations.....	57
Figure 4-6 Kinetics of CMS and ES reacted after polymerization with styrene. The smooth curves represent the pseudo-first-order equation fit and the data points represent the experimental observation.....	61
Figure 4-7 Kinetics of styrene reacted for different feed concentration. The smooth curves represent the pseudo-first-order equation fit and the data points represent the experimental observation.....	63
Figure 4-8 Influence of monomer feed concentration on graft length. Polymerization reaction time was 120 minutes.....	65
Figure 4-9 Effect of initiator reaction time on amount of styrene reacted.....	67
Figure 4-10 Effect of initiator reaction time on graft length.....	68
Figure 4-11 Effect of initiator reaction time and monomer feed concentration on IEC.....	70

CHAPTER 1

INTRODUCTION

1.1 Technological background

Packed bed chromatography is the most common downstream process in the biotechnology industry for separation of proteins and antibodies [1-3]. Although this process provides an excellent degree of purity and reproducibility, there are areas which need improvement such as high cost and low-throughput [4]. Scale up to large diameter chromatography columns presents numerous problems include process complexity, high cost, and complex process control required to achieve good isolation of biological molecules (enzymes, proteins and antibodies). Therefore large scale purification of proteins and antibodies is a major challenge faced in downstream processing of biotechnology industry. Membrane chromatography is an excellent option to lower cost and improve throughput [4-9]. Mass transfer in membrane chromatography is dominated by convection, resulting in reduced processing times and higher throughput [10]. However, in spite of the advantages of membrane chromatography, there are major challenges that need to be addressed for its broader implementation. These include improved equilibrium binding capacity, selectivity, uneven membrane thickness, pore size distribution, and flow distribution [4, 11-12]. This research addresses the problems of low binding capacity and selectivity associated with membrane chromatography by using functionalized membranes.

Functionalized membranes have polymeric adsorptive sites immobilized in the pores of the membrane. Polymer grafts can be formed by permeating a solution of monomer through the pores of the membrane. Each graft contains multiple binding sites, resulting in improved equilibrium binding capacity. Homopolymers and block copolymers were synthesized in the

pores of microfiltration membrane (0.22 μm pore size) composed of polyethersulfone (PES) [13]. The grafts are formed by cationic polymerization of styrene and substituted styrene monomers CMS and ES. Figure 1-1 (a) shows the PES membrane cross section including the membrane pores and the shaded solid region. The pores of membrane contain multiple polymeric grafts. Zooming in the pores, a representative polymeric graft is shown in the Figure 1-1 (b). Each polymeric graft has multiple binding sites shown as a combination of series of “D” shapes and a straight line. The binding site adjacent to the initiator (immobilized on PES backbone shown as shaded in the Figure 1-1 (b)) is further zoomed in to show the pattern of each binding site in Figure 1-1 (c). Each binding site has heterogeneous functional groups (phenyl, hydroxyl and chloromethyl) derived from monomers styrene, ES and CMS.

The formation of block copolymers (styrene-co-ES and styrene-co-CMS) is the first step in creating a synthetic analog of the dipeptide structure phenylalanine/tyrosine (Figure 1-2) in protein A ligand. It has been shown in the literature that this structure is very important for binding with the Fc region of antibody IgG [14-15]. Styrene-co-ES (post hydrolyzed) block copolymer will give side chain functionalities similar to phenylalanine and tyrosine residue and CMS will be used to attach spacer units to prevent antibody denaturing and steric hindrance during adsorption. Additionally these spacer units will inhibit sorption of bovine serum albumin when competitive sorption studies will be performed in the future.

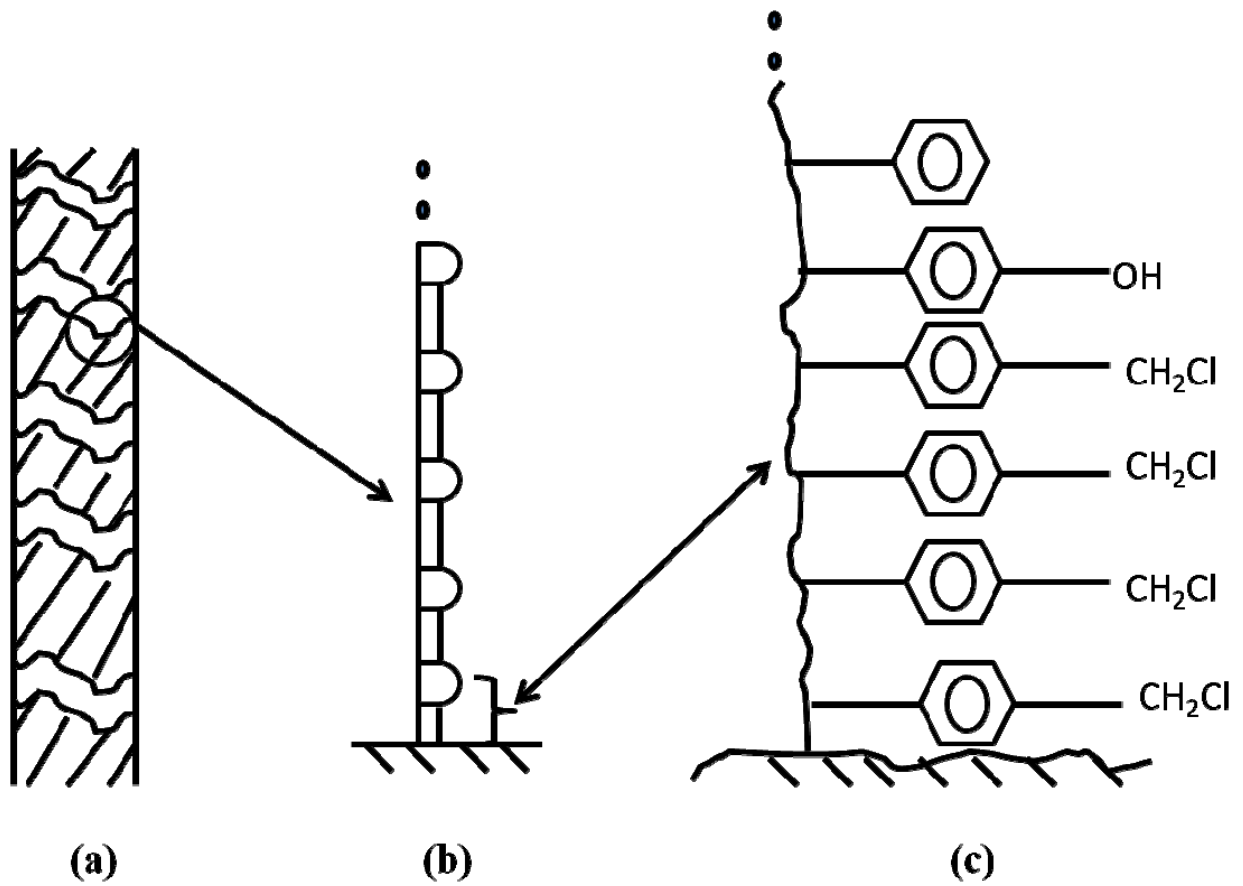


Figure 1-1. Schematic of (a) PES membrane cross-section; (b) representative polymer graft; and (c) heterogeneous binding site.

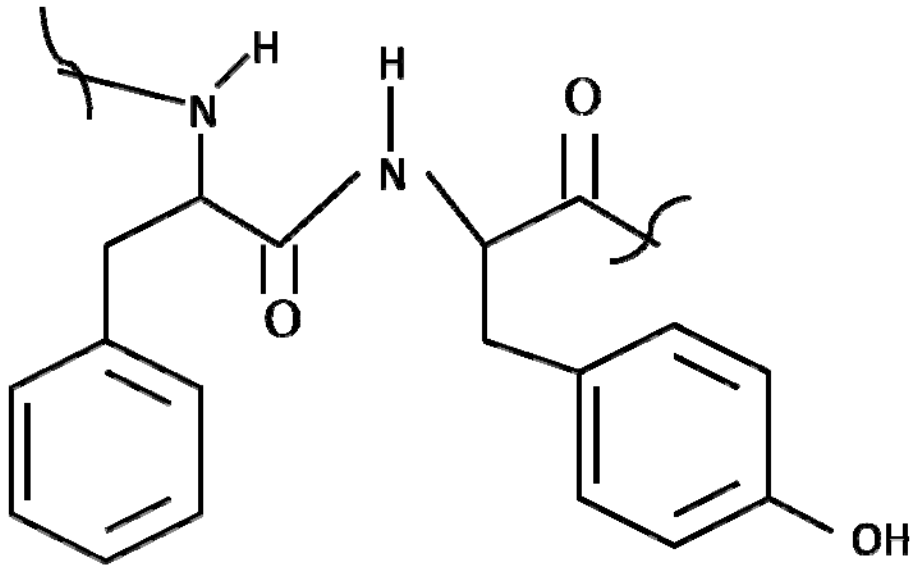


Figure 1-2. Phenylalanine-tyrosine dipeptide structure.

1.2 ImmunoglobulinG (IgG) and Protein A binding chemistry

The structure of IgG (150 kDa) consists of four peptide chains, two identical heavy chains (50 kDa) and two identical light chains (25 kDa). The heavy chain is connected to the light chain and the other heavy chain by disulfide bonds. Each heavy chain contains one variable domain (V_H) and three constant domains (C_{H1} , C_{H2} and C_{H3}). The region between the C_{H1} and C_{H2} domains is the hinge region, where the antibody molecule arms form a flexible Y shape. The antibody hinge region structure controls the biological profile. The Fragment antigen binding (Fab) segment contains the antigen-binding site, and the Fragment crystallizable (Fc) segment has high affinity for Protein A [Figure 1-3] [14].

The structure of Protein A can be broadly divided into two parts. The first part consists of three alpha helices arranged in an antiparallel bundle. The second part consists of 72 different chains composed of essential amino acids like leucine, lysine, aspartic acid, phenylalanine, and tyrosine. Among these different chains of amino acids, the particular dipeptide structure of Phenylalanine-Tyrosine (Figure 1-2) is very crucial for interaction with IgG [15]. The dipeptide structure is similar to the Fc receptor (protein) which binds specifically to the Fc region of the antibody due to complementary binding sites. The three-helix bundle of Protein A does not take part in interaction with IgG. In this research we will create a synthetic analog of phenylalanine/tyrosine dipeptide structure of Protein A inside the pores of microfiltration polyethersulfone membrane by sequential cationic polymerization of styrene and substituted styrene monomers. In the subsequent sections, research objectives and the approach to create block copolymers will be discussed.

1.3 List of research objectives

The overall objective of this research is to synthesize and characterize homopolymer and block copolymer brushes in microfiltration polyethersulfone membranes formed by cationic polymerization of styrene and substituted styrene monomers. This goal is realized through the following steps.

1. Form initiators (sulfonic acid groups) for cationic polymerization of styrene and substituted styrene monomers (CMS, ES) in the membrane pores.
2. Determine IEC of sulfonated and grafted membrane.
3. Synthesize homopolymer brushes using styrene and substituted styrene monomers.
4. Synthesize block copolymer (styrene-CMS, styrene-ES) grafts through sequential polymerization of substituted styrene monomers.
5. Study flux versus pressure drop to quantify permeability of raw, sulfonated and grafted membrane.
6. Study of controlled polymer growth. Polymer growth aspects like kinetics of monomer reacted, ion-exchange capacity (IEC), and graft length were studied with respect to parameters such as initiator contact time and monomer feed concentration.
7. Thorough quantification and characterization of polymer grafts with analytical techniques like UV spectroscopy, atomic absorption and gas chromatography.

1.4 Approach

In this work, the processes to immobilize initiator and form grafts by sequential cationic polymerization to add multiple specific adsorption sites were examined. In this work, homopolymer and block copolymer grafts are formed in the pores of microfiltration PES membrane. Initiators in the form of sulfonic acid groups were immobilized in the pores of the membrane by a simple chemical reaction. This is followed by polymerization with the monomer. This is a living polymerization, where the reaction is limited only by the availability of the monomer. In general, the experimental tasks performed are ion-exchange studies, quantification of polymer grafts, permeability studies and kinetic studies. Figure 1-4 shows the breakdown of the approach to perform these tasks.

Commercially available microfiltration PES membrane was modified by sequential cationic polymerization of styrene and substituted styrene monomers (CMS and ES). Homopolymer and block copolymers were formed in the membrane pores. Permeability studies at each stage were performed to give preliminary evidence of formation of grafts. IEC of sulfonated and grafted membrane was determined after each stage of modification. Polymer grafts were quantified and characterized using analytical techniques like UV-vis analysis and gas chromatography. Finally, kinetics of polymerization reactions were studied to understand controlled polymer growth.

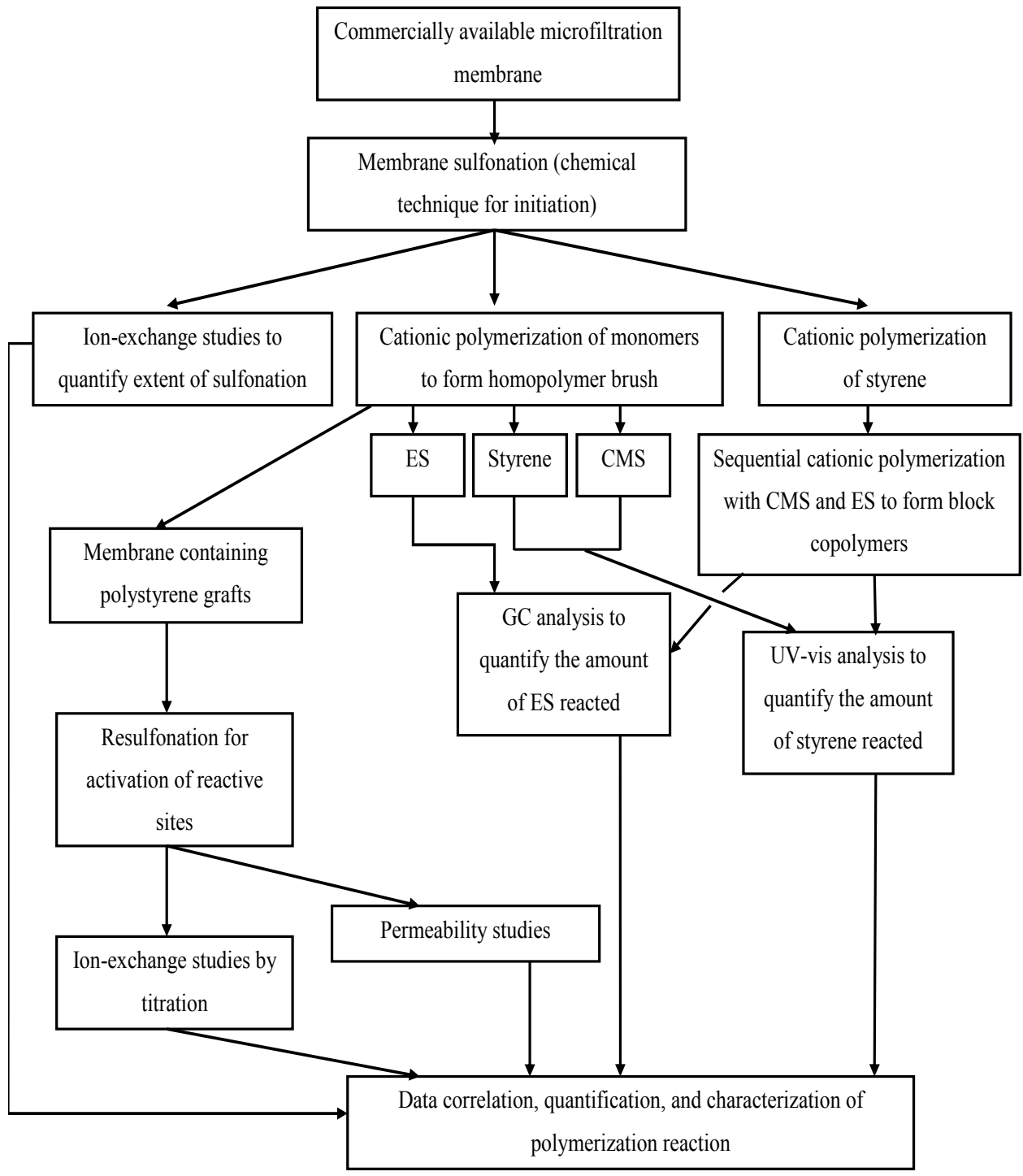


Figure 1-4. Experimental approach for functionalization of PES microfiltration membrane.

CHAPTER 2 BACKGROUND AND THEORY

2.1 Introduction

This research is primarily focused on synthesis and characterization of homopolymer and block copolymer grafts in the pores of microfiltration polyethersulfone membranes. The purpose of formation of block copolymer grafts is to create a synthetic analog of ligands in affinity chromatography. The results of this research will improve fundamental understanding of functionalized membranes and controlled polymer growth. The research will also provide insights into dynamic and equilibrium binding capacities of functionalized membranes. One unique aspect of this work is to create multiple specific interaction sites having different functional groups in the pores of the membrane. This will help in synthesizing customized structures for applications such as protein separation. Additionally, it will expand the use of functionalized membrane as membrane adsorbers for membrane chromatography. In order to gain a better understanding of this work, it is essential to know the background of monoclonal antibodies, affinity chromatography, membrane chromatography, affinity membranes, functionalized membranes, polymer brushes, and chemical techniques for immobilization of multiple specific interaction sites built into a polymer brush structure. Reviewing the theory and research work in all these areas will form a better understanding of this technology.

2.2 Monoclonal antibodies (MAbs)

2.2.1 Definition

Monoclonal antibodies are monospecific antibodies made from identical immune cells that are all clones of a single hybrid cell [16]. Immune cells are involved in defending the body against bacteria, viruses, diseases and other foreign invaders like parasites. The first important

characteristic of MAbs is they are extremely specific; that is, each antibody binds to and attacks one particular antigen (virus, disease-causing bacteria, and infectious agent). Second, antibodies once formed against a particular disease continue to offer resistance against that particular disease, such as antibodies formed against measles and chickenpox.

2.2.2 Applications of MAbs

MAbs have a variety of applications ranging from academic, medical and commercial uses. MAbs can be used to characterize cell surface proteins which will help in understanding biological functions of membrane proteins. For example, MRK16 (IG₂ isotype) and MRK17 (IG₁ isotype) were used to detect membrane antigens [17]. Antibodies are used in the radioimmunoassay and radio immunotherapy of cancer, and some new methods can even target only the cell membranes of cancerous cells. An excellent example is MAbs developed against ovarian cancer. Human monoclonal antibody TC5 (immunoglobulin G1) specifically targets ovarian cancer cells and does not react with normal organs like the liver, heart, lung, or pancreas [18]. MAbs can be used to treat viral diseases like AIDS. A combination dose of two monoclonal antibodies, MAbs 2F5 and 2G12, has been successful in neutralizing HIV virus [19]. MAbs also have successful applications in organ transplants. OKT3, a murine antibody linked to the T-cell antigen receptor cells, is used in clinical applications to prevent and treat acute organ rejection [20]. With such a wide range of applications requiring MAbs doses ranging from milligrams to grams, there is a lot of commercial interest to scale-up MAbs production for therapies requiring larger doses. Hence, large scale purification of monoclonal antibodies has generated great commercial interest.

2.2.3 Purification of MAbs

Antibody purification can be divided into two main groups: precipitation methods and chromatographic methods. Typically the precipitation technique is used in downstream processing (recovery and purification of biological products) preceding other chromatographic steps to increase product purity. Sodium sulfate or ammonium sulfate salts can be used to precipitate the antibodies. Antibodies can also be precipitated using ethanol or by electrolyte depletion [21]. Chromatographic methods are classified as non-affinity and affinity based. Affinity chromatography is the most common method for antibody purification and its principle and limitations will be described in the following section. The research in this thesis is focused on addressing the limitations of affinity chromatography using functionalized membranes as membrane adsorbers in membrane chromatography for large scale purification of MAbs.

2.3 Affinity chromatography

Affinity chromatography is the critical separations component of downstream processing in the biotechnology industry [1-2, 22-26]. This technique is the most common method for separation of proteins and antibodies. Affinity chromatography is effective, but expense and low throughput complicate large scale operation.

2.3.1 Principle

Affinity chromatography is a method of separating proteins and antibodies from biochemical mixtures (e.g. blood serum) and is based on a highly specific chemical interaction between the solute and ligand [27]. The stationary phase typically consists of a silica or agarose gel containing a surface ligand to bind the protein [28]. The stationary phase should have good chemical and physical stability, flow and packing characteristics, and functionalities for binding a wide variety of compounds. The process starts with a solution (cell lysate or blood serum)

containing different types of molecules passed through the stationary phase in an affinity column. The molecules of interest have a specific property that will bind with ligand on the immobilized (stationary) phase. Solid medium (stationary phase) is then removed from packed column and specific molecules of interest are eluted from the medium.

2.3.2 Applications

The most common use of affinity chromatography is preparative separation of proteins and antibodies [29-32]. The application of affinity chromatography for the elimination of undesirable substances from the blood of living organisms is also being investigated [33]. Affinity chromatography can be used to study the possibility of substituting natural peptide chains of enzymes with various modified synthetic peptides [34]. Enzyme solutions are purified and concentrated by affinity chromatography which helps in determining interactions between biological compounds and drugs [34]. A detailed review of clinical applications of affinity chromatography was published by Hage [3]. In this review, applications were grouped based on the type of ligand. For example, boronic acid was used as ligand for determination of glycohemoglobin for the assessment of long term diabetes. Another example is the use of lectin as a ligand to bind certain types of carbohydrate residues [3]. In all the applications discussed, the type of ligand plays a very important role and will be discussed in the subsequent section.

2.3.3 Ligands in affinity chromatography

The application of affinity chromatography for large scale production is limited by the low availability of suitable ligands for scale-up. Other challenges include ligand stability, high selectivity, short process times and high cost. These problems have been addressed in recent years by rational and combinatorial approaches to design low cost, stable, and highly selective synthetic affinity ligands [31, 35-37]. Ligand design has been made more feasible and faster by

using combined knowledge of advanced computational tools and protein structure with defined chemical synthesis [31]. New synthetic affinity ligands have been synthesized by combinatorial approaches based on libraries of peptides and nucleic acids [36, 38]. In the following paragraphs different types of natural and synthetic ligands for affinity-chromatographic purification of antibodies and their advantages/disadvantages will be discussed.

2.3.3.1 Affinity ligands for immunoglobulins

The immunoglobulins can be divided into five different classes, namely: IgG, IgA, IgE, IgM and IgY. Proteins A or G are the common affinity ligands for purification of IgG and IgM [39-40]. Though these are the most common affinity ligands for purification of the majority of antibodies, there are cases where they have shown ligand leakage (shedding of ligand from support matrix), poor affinity and low binding capacity. Fuglistaller [39] reported ligand leakage with different protein A column matrices using mouse monoclonal IgG3 antibody. It was shown that there was significant leakage at pH 4 in presence of IgGs and at pH 8.9 in absence of IgGs. Protein A showed low affinity to affinity purified canine IgG and IgM using a protein A-agarose column [41]. Proteins A or G do not recognize IgM from sera or cell culture [31]. Alternatively, mannan-binding protein (MBP) has turned out to be a viable option for purification of IgM. Mouse monoclonal IgM purified by this method is 95% pure. However, the binding capacity is limited to 1 mg/ml and the isolation from rat liver is complex, time consuming and expensive [42].

IgA can be purified by fractional precipitation, zone electrophoresis, ion-exchange and other chromatographic procedures [43-44]. Combination of ion-exchange chromatography and immunoabsorption has been successfully used to purify IgA from human serum. Commercially available anion-exchange cellulose was used to isolate IgA. Propionic acid was used as a ligand

in sepharose columns. The purity of the product was greater than 99%. However, the process required an additional immunoadsorption step to reduce contamination from IgG to less than 1%. Additionally, it has been reported that functionality of IgA may be altered if higher concentrations (1M acetic acid containing 4M urea) of eluants are used to improve recovery [45].

IgE can be purified by immunoaffinity chromatography using anti-IgE antibodies [46-47]. However, ligand leakage greater than 20 ppm from immunoaffinity columns with glucagon antibodies has been reported [48]. The ligand leakage from commercially available protein A based affinity medium MabSelect SuRe is less than 3 ppm. Other approaches to purify IgE include ion-exchange and size exclusion chromatography [49]. Studies carried out to investigate binding of proteins A and G for human IgE revealed that protein A showed 12-14% binding with serum polyclonal IgE. However, protein G showed no binding with IgE [50].

IgY, which is typically found in egg yolk, is difficult to isolate because it is present in the water soluble fraction which contains dispersed lipid fraction. Common affinity ligands like Protein A or G showed no binding for IgY [51-52]. Thus issues like poor affinity, low selectivity, high cost, time consuming procedures, alteration in functionality, ligand leakage and incompatibility for industrial scale-up opens up opportunities to investigate novel ligands that address these limitations.

2.3.3.2 Synthetic (Biomimetic) ligands

One alternative to address the limitations of conventional ligands is the development of synthetic ligands. The advantages include low cost, resistance to chemical and biological degradation, high specificity, high capacity (up to 40 mg protein per ml adsorbent), large scale use (columns > 100 liter) and high sterilizability [53-54]. In recent years, advanced computer-

aided molecular design and combinatorial chemical techniques have been used to synthesize and design ligands that mimic their biological counterpart [55-57].

A peptide library comprising 88 ligands was screened to find a ligand which shows binding with pure human IgG [57]. It was found that 3-aminophenol and aminonaphthol substituted on a triazine nucleus was highly effective in binding human IgG showing purity greater than 99%. The binding capacity was observed to be 51.9 mg/g moist gel, and 60% of human IgG from plasma was separated [32, 57]. Protein A mimetic (PAM), also known as TG19318 (Figure 2-1), is another novel synthetic ligand designed by screening of the synthetic peptide library by computational tools. The tetramer of a tripeptide (Arginine-Threonine-Tyrosine), identified after three cycles of screening using computer simulation, showed binding with the Fc portion of IgG. It was then immobilized on preactivated solid supports (enzyme-linked immunosorbent assay format). It was reported that purification of antibody was approximately 95%. Additionally, the ligand was found to be stable and there was no detection of leaks in the purified stream [58]. It is used to purify mouse monoclonal IgE and IgG. The binding capacity can reach up to 5 mg IgE/ml of the support, and 25 mg IgG/ml of the support, respectively [32, 59].

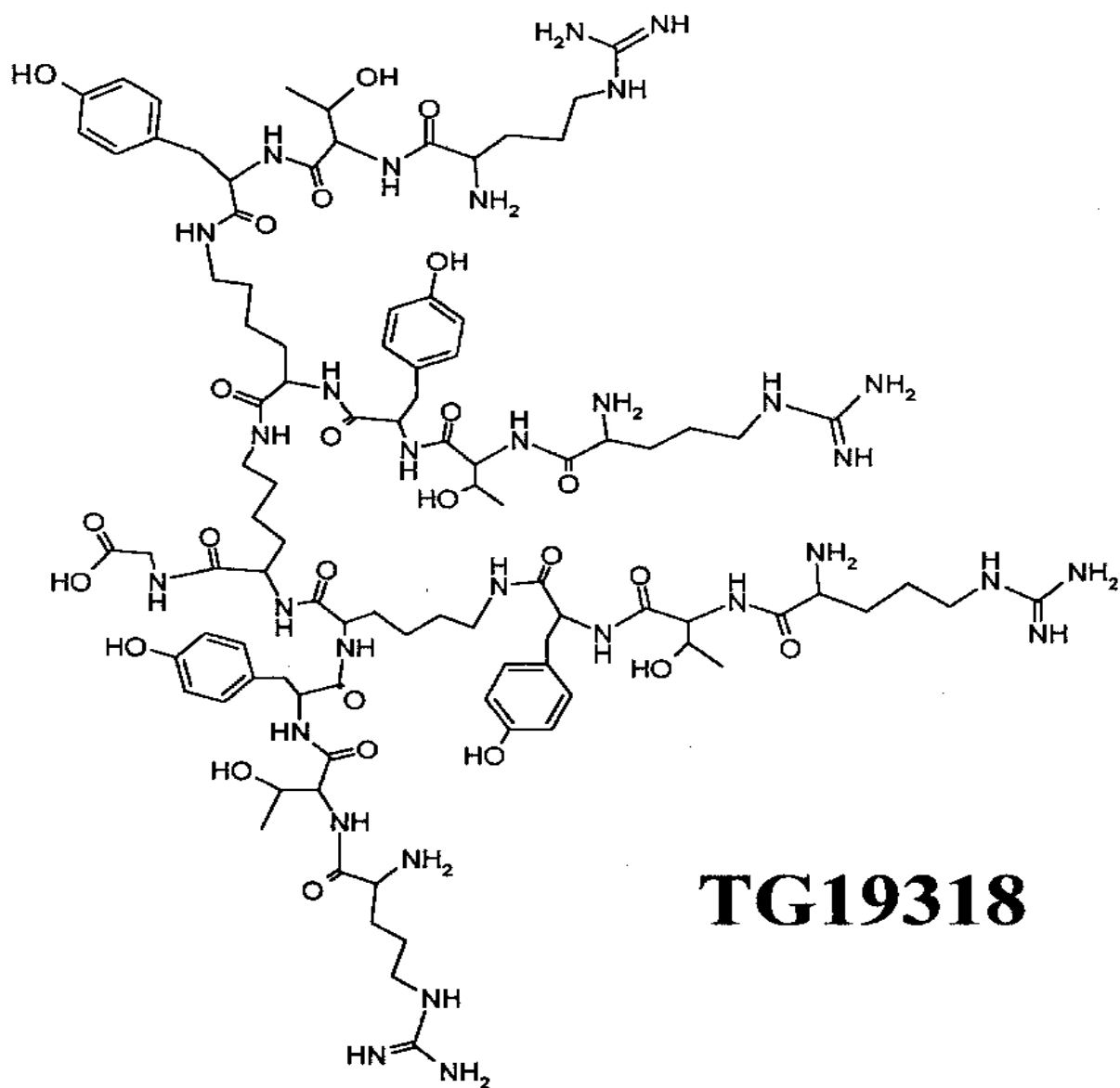


Figure 2-1. Chemical structure of TG19318 [60].

Artificial protein A (ApA) was designed and synthesized to mimic the protein A dipeptide structure Phe132-Tyr133 responsible for IgG binding. Computer aided molecular modeling was used to mimic the dipeptide structure. Stability of the adsorbent was tested with 1M NaOH and the capacity was unchanged following treatment in five cycles. ApA showed a selectivity of 98% for IgG as compared to 94% for biological protein A. Another measure to describe affinity between two molecules is the equilibrium constant that describes bonding affinity between two molecules. The lower value indicates high affinity between molecules. The affinity constant between ligand ApA and IgG was approximately one-thousandth of the affinity exhibited between biological protein A and IgG. Additionally, the binding capacity between ApA and IgG was found to be 20 mg IgG/g moist gel [61].

2.3.4 Limitations of affinity chromatography

Although affinity chromatography is effective and provides excellent resolution and reliability, there are a number of drawbacks. First, the pressure drop across a packed chromatography bed is generally very high, in the range of 20-90 bar [62-63]. High pressure drop deforms the spherical particles in the packed bed. These particles accumulate and blind the bed, further limiting the flow rate [64]. Second, transport of solute particles to their corresponding binding sites takes place by intra-particle diffusion. This results in increased process time and recovery volumes (elution volume). Third, channeling due to cracking of the packed bed causes a tremendous loss in loading capacity (amount of protein bound to substrate) [4]. Fourth, ligands and products are exposed to harsh elution conditions for long times which increases the chances for denaturation. Fifth, separation of macromolecules by affinity chromatography is often a problem since large size protein molecules cannot enter the small

pores of particles in a packed bed. Sixth, the most common ligands used in affinity chromatography are still from biological origin. This makes these ligands very expensive and purification steps are required before the ligand is bound to the stationary phase. Finally, mass transfer limitations cause problems with scale-up such that large scale purification (grams per patient per year) of proteins and MAbs is very expensive. Therefore, there arises a need for new a separation technology which addresses the limitations of affinity chromatography [5, 65-66].

2.4 Membrane chromatography

An alternative viable technology to overcome the limitations associated with affinity chromatography is to use synthetic microporous or macroporous membranes as chromatographic media [5-9]. Membrane chromatography is a more recent purification technique designed to avoid the fundamental limitations of columns packed with beads [4, 67]. The membranes used in membrane chromatography contain functional ligands attached in the pores as adsorbent sites.

2.4.1 Advantages over affinity chromatography

Membrane chromatography is dominated by convective mass transfer, resulting in high dynamic binding capacity, high productivity and reduced processing times (Figure 2-2). The elimination of diffusional resistance minimizes some of the problems of affinity chromatography like process time (one-tenth the time taken for packed beds) and intra-bed diffusion [9, 68-69]. The result is exceptional throughput, good resolution (membrane stacks), and higher dynamic binding capacity than packed beds. Furthermore, the cross-sectional area of the membrane bed relative to bed length is much larger as compared to affinity columns. Hence, the pressure drop is drastically reduced resulting in higher flow rates and thus higher productivities [70-74].

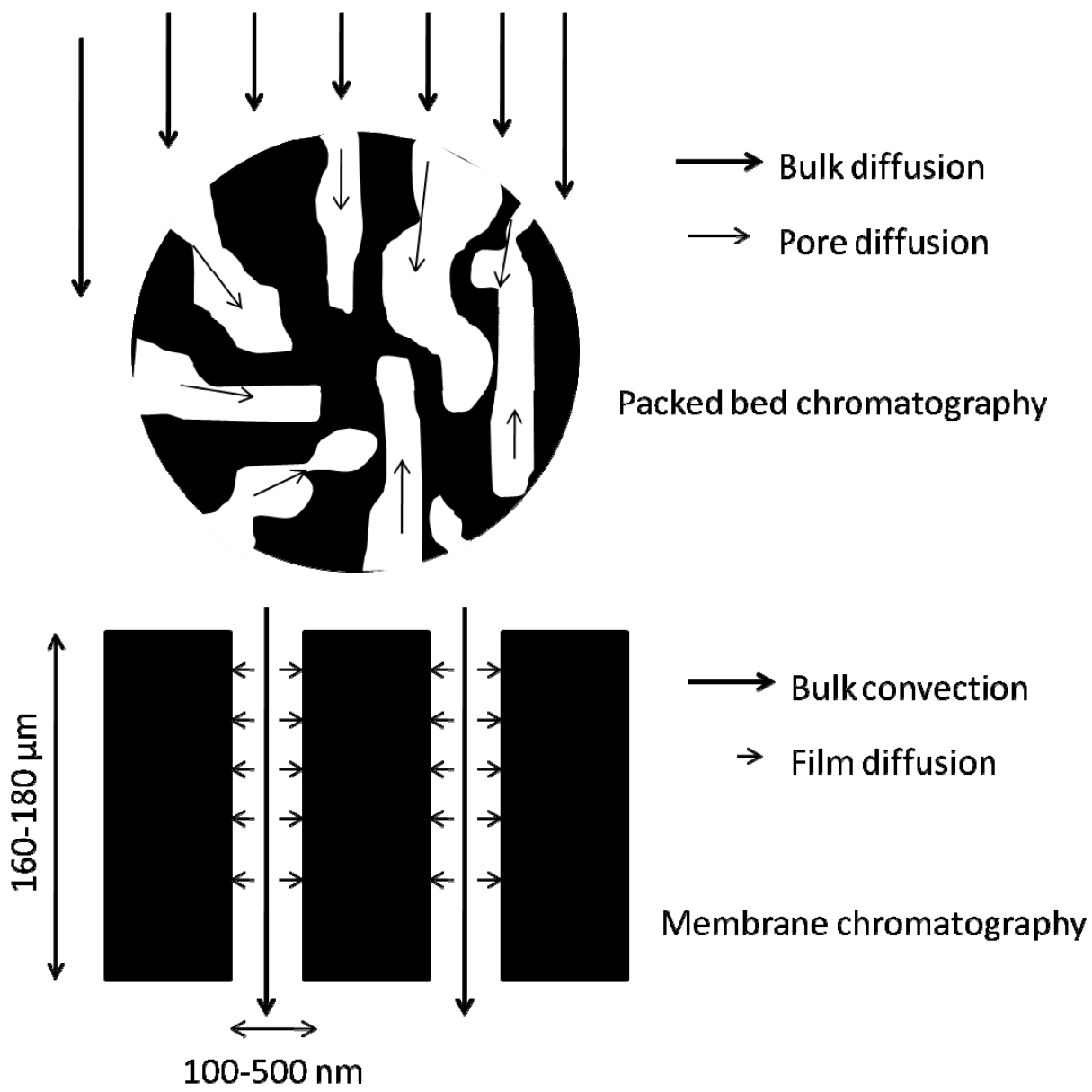


Figure 2-2. Solute transport in membrane and packed bed (pore diameter 100-200 nm) chromatography [4].

Membrane chromatography can be used for separating large size protein molecules of molecular weight greater than 250 kDa. This is because large size proteins have access to much higher binding internal surface area due to the macroporous support nature [75-76]. In the work of Yang et al. [77], the dynamic binding capacity of thyroglobulin (20 nm diameter) was reported to be 10 ± 2 mg/ml as opposed to 3 ± 0.8 mg/ml for alpha-lactalbumin (3.5 nm diameter) using an anion-exchange membrane (Q membrane). This corresponds to 160-200% increase in dynamic binding capacity for large size molecules as compared to small size protein molecules. Additionally, low production cost allows development of disposable membrane adsorbers when properties such as binding capacity, selectivity and permeability drop below separation efficiency. Scale-up is a relatively straightforward procedure because capacity is linearly dependent on the membrane surface area (or volume) as well as the size of membrane unit. However, this potential has not been fully capitalized for large scale separation of proteins and antibodies. Lightfoot and coworkers [12] reported that scaling up to larger support diameters reduces the separation efficiency and can cause inefficient flow distribution. Hence, there remain several technical challenges to broader implementation of membrane chromatography.

2.4.2 Affinity membranes for protein purification

Affinity membranes were developed to address the limitations of affinity-based purification with packed beds. Affinity membranes are composed of grafted functional groups (ligands) that are anchored in the pores of a microfiltration membrane. The types of functional groups employed include amino acids, biological ligands, metal affinity ligands, ion-exchange ligands, and antigen and antibody ligands. In subsequent paragraphs, ligands and matrix performance will be discussed.

A hollow-fiber affinity membrane containing phenylalanine or tryptophan ligands was prepared by grafting glycidyl methacrylate onto a porous polyethylene membrane by radiation-induced grafting [78-79]. Bovine γ -globulin saturation capacities of affinity membrane with phenylalanine and tryptophan ligands were 36 and 49 mg/g, respectively. Residence times ranging from 55-220 seconds confirm negligible mass transfer resistance. Protein A and protein G immunoaffinity membranes have also been used to purify IgG at low residence times. IgG was purified in only 10 minutes in a single pass at high flow (150 cm³/min) and low pressure drop 0.83 bar as compared to 20-90 bar in affinity chromatography [80, 62-63]. Immunoaffinity membranes immobilized with proteins have shown binding capacities similar to that of a packed column. Protein A was immobilized on hollow fiber membranes composed of modified polysulfone to adsorb IgG [81]. The highest binding capacity studied was comparable to that of bead matrices.

Immunoaffinity membranes have potential use in clinical apheresis (separation of different constituents of blood) applications [82]. The affinity ligand L-histidine was immobilized onto poly (ethylenevinyl alcohol) hollow fiber membranes for selective removal of human IgG from plasma or serum *in vitro*. The pseudobiospecific affinity membrane showed higher capacity than protein A membrane. Additionally, the membrane had higher affinity for IgM as compared to other immunoglobulins (IgA and IgG) studied. Due to lower cost (less expensive ligand), high capacity, specificity and stability of histidine affinity membrane it has a potential for large scale application.

Immobilized metal ion chromatography affinity membrane also showed improved flow rates as compared to packed beds [83]. S-oxynitrilase was purified from Sorghum bicolor using immobilized iminodiacetic acid (IDA)-copper ion membrane. The membrane showed a 200-fold

increase in flow rate as compared to a gel. However, the binding capacity of 0.15 mg of S-oxynitrilase per cm^2 was slightly lower than the gel.

As discussed above, affinity membranes have clear advantages over conventional packed bed chromatography in terms of cost, residence time, and flow rate. However, there are areas which need improvements for large scale production. This will be discussed in the following section and how this research will be helpful in addressing some of these challenges.

2.4.3 Challenges for improvement in membrane chromatography

Undoubtedly, separation by membrane chromatography has several advantages over packed bed chromatography. However, some of the major challenges of membrane chromatography include lower equilibrium binding capacity, membrane pore size distribution, selectivity, and uneven membrane thickness. Suen [84] reported that a porosity variation of 3% can result in 11% loss in loading capacity. The pore size in macroporous membranes is usually represented as a range since all the pores are not of the same diameter. This wide pore size distribution results in the feed preferentially being carried through the larger pores, with very little flow through the smaller pores. As a result, utilization and hence the efficiency of the adsorbent is reduced. Variation in porosity also causes channeling leading to loss in loading capacity. Membrane thickness often ranges from several hundred to thousands of microns in a stack and hence due to this wide range there is often nonuniformity in thickness. The adsorbent utilization may be reduced as a result of uneven membrane thickness; flow is usually greater where the membrane is thinner due to the lower pressure drop. Suen [84] reported that a 10% change in membrane thickness results in 10% loss in loading capacity. Binding capacity of membrane adsorbents is lower due to lower surface area to bed volume ratio as well as non uniform inlet flow distribution. The loss of internal surface area generally results in a decrease in

the equilibrium binding capacity. Functionalized membranes synthesized in this research have polymeric grafts with multiple binding sites extending into the pore; therefore, sorption capacity was increased by several orders of magnitude.

Although membrane chromatography appears to be an ideal candidate for large-scale purification and recovery of proteins and enzymes, its potential has not been fully utilized in biotechnology industry. Proper distribution of inlet flow is one area which needs to be investigated in detail. Clearly, the equilibrium binding capacity, pore size distribution, selectivity and flow distribution must be improved if membrane chromatography is to meet the future separation needs of the biotechnology industry.

2.5 Functionalized membranes

2.5.1 Principle

One advance that has resulted in improved equilibrium binding capacity is the development of functionalized membranes. These are membranes where polymers containing adsorptive sites are immobilized in the pores. The grafts may be formed by polymerization from the monomer, or by attachment of large chain molecules, such as enzymes and polyamino acids [85-86]. In most cases, functionalization results in the addition of a polymer brush in the pores of the membrane, where active sites for adsorption are located in the membrane flow path. The surface chemistry of the membrane is altered to carry out polymerization, affecting its intrinsic properties such as permeability, separation capability, and conductivity. In most cases, the membrane backbone matrix acts as a stable skeletal support for grafted polymers. In the case of porous polymer membranes, the porous structure gives an opportunity for polymer graft stability by providing sufficient interaction between the membrane and the grafted polymer.

2.5.2 Introduction to polymer brushes

Polymer brushes are defined as layers or assemblies of chains end-tethered (grafted, anchored) to a surface or interface [88-90]. The interface to which polymer brushes are grafted may be a solid substrate surface, the interface between liquid and air, or the interface between two liquids. Tethering of polymer on a solid substrate can take place either chemically or by physical adsorption. There are three methods for synthesizing polymer brushes. These include grafting to, grafting from and grafting through. Among these, grafting to and grafting from are the most common. In grafting to method, polymer chains with functional end groups diffuse through the surface which has complimentary functional groups. A reaction then takes place between the functional groups on the surface and polymer. As a result, polymer chains will be tethered on the surface. In grafting from method, an appropriate initiator is attached first and then monomer is diffused through a solid surface at appropriate polymerization conditions. Monomer reacts with the initiator and polymer chains grow from the surface. The advantage of grafting from is that multiple grafts can be formed which increases the binding capacity, and the growth of the grafts can be controlled to create a customized structure.

2.5.3 Classification of polymer brushes

Polymer brushes based on chemical composition can be classified into homopolymer, mixed polymer, random copolymer and block copolymer brushes (Figure 2-3). Homopolymer brushes (Figure 2-3 ($a_1 - a_4$)) consist of one type of monomer molecule. In mixed polymer brushes (Figure 2-3 (b)), two or more different monomers are grafted to the same substrate [91]. Random copolymer brushes (Figure 2-3 (c)) consist of two different monomer molecules randomly distributed along the polymer chain [92].

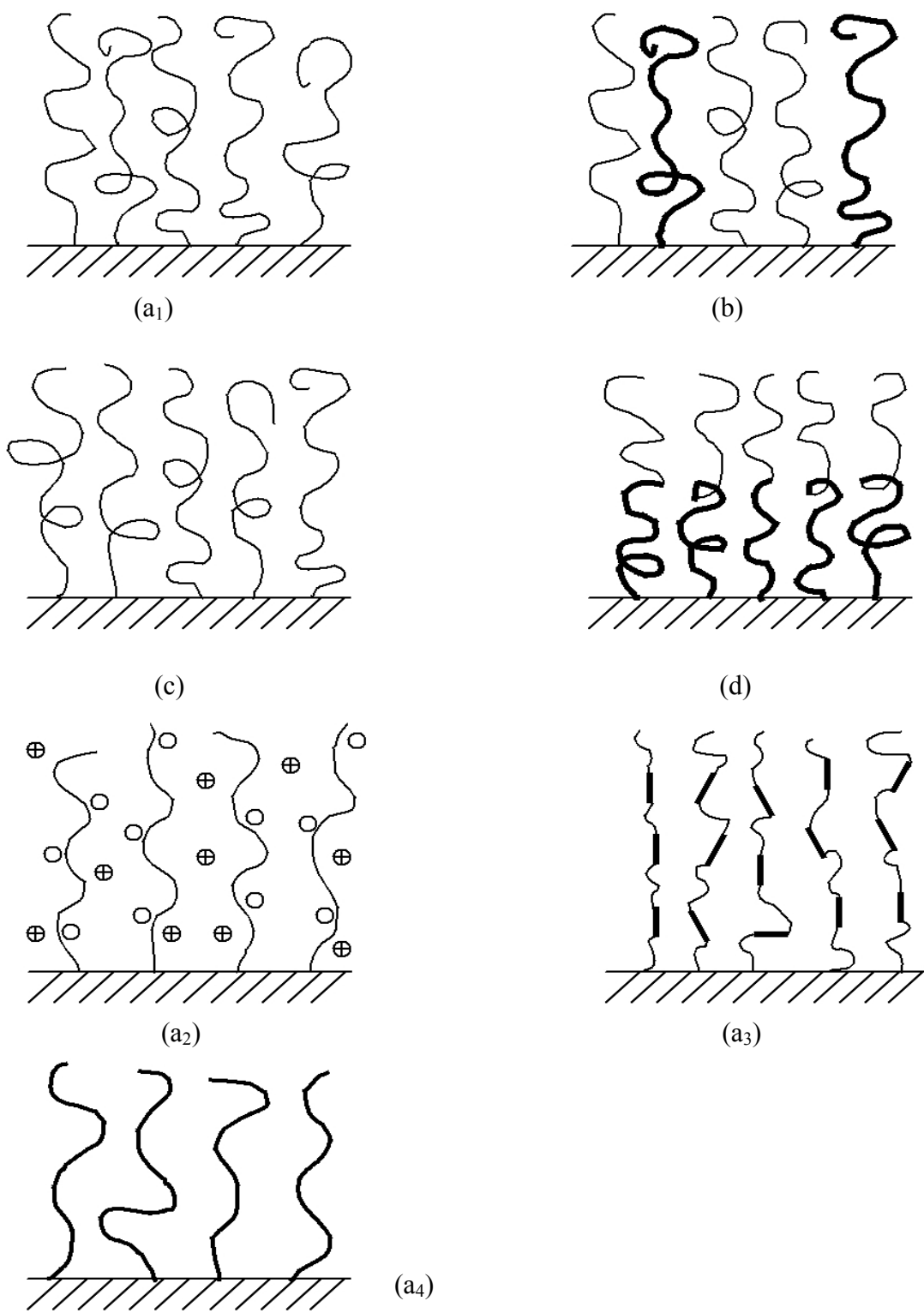


Figure 2-3. Classification of linear polymer brushes: (a₁ -a₄) homopolymer brushes, (b) mixed polymer brush, (c) random copolymer brush, and (d) block copolymer brush [93].

Block copolymer brushes (Figure 2-3 (d)) consist of two or more monomer chains linked by covalent bonds [94]. Homopolymer brushes can also be classified based on their polarity and these include neutral and charged polymer brushes (a_2). Another way of classifying homopolymer brushes is in terms of stiffness of the polymer chain and that includes flexible/semi-flexible (a_1, a_4) and liquid crystalline polymer brushes (a_3).

2.5.4 Graft polymerization by chemical techniques

Many methods for graft polymerization of different monomers on polymers have been developed. These techniques include chemical, photochemical, radiation induced, plasma induced and enzymatic grafting. Chemical grafting techniques will be discussed in the subsequent paragraphs. The discussion of other techniques is beyond the scope of this thesis.

Grafting by chemical means can be classified into two types: free radical and ionic. In grafting through free radical polymerization, free radicals are produced from the initiator and transferred to the substrate to react with the monomer to form the graft copolymer. Grafting through ionic polymerization can further be classified into cationic and anionic polymerization. The initiators for cationic polymerization are electrophilic agents which are electron acceptors; the common examples are sulfuric acid and hydrochloric acid. Additionally, the compounds which generate carbenium ion can also be used as initiator [95]. Anionic polymerization is a form of addition polymerization that involves the polymerization of vinyl monomers with electronegative groups [96]. This polymerization is carried out through a carbanion active species. The polymerization through ionic mode can be living which means polymerization occurs until all the monomer molecules are exhausted or until a desired molecular weight is achieved for particular application.

Functional groups such as carboxyls, phenyl, sulfonic acid, hydroxyls, amines, halogen, and double bonds may be attached to the living active centers [97-99]. The versatility of the method allows placing these functional groups at any position, either at the beginning, middle or end of polymers, between blocks or evenly spaced along polymer chains. Castro and coworkers introduced vinyl groups chemically by grafting polyvinyl-pyrrolidone brush on porous silica membranes [100]. Ritchie and coworkers [101-102] have successfully immobilized multiple reactive groups (COO^- , NH_3^+ , and SH) on cellulose or silica based membrane by chemical techniques. In this work, the functionalization of polymer grafts is accomplished by cationic polymerization of styrene and substituted styrene monomers (CMS and ES). Sulfonic acid groups (SO_3^-) immobilized in the pores of the microfiltration membrane act as initiator for cationic polymerization.

2.6 Cationic polymerization

Cationic polymerization is a type of chain growth polymerization in which the active end of a growing polymer molecule is a positive ion. Protonic acids, for example sulfuric acid, can be used as initiators in cationic polymerization. The proton from an acid (HA) is transferred to a monomer molecule (M) giving HM^+ cation and A^- counterion. The newly formed cation will further react with other monomer molecules, each time forming a cation. Molecular weight increases with formation of polymeric grafts. This process is repeated until all the monomer molecules are used up, and thus cationic polymerization is a living polymerization [100]. Figure 2-4 illustrates the propagation step of the reaction mechanism for styrene polymerization in a membrane.

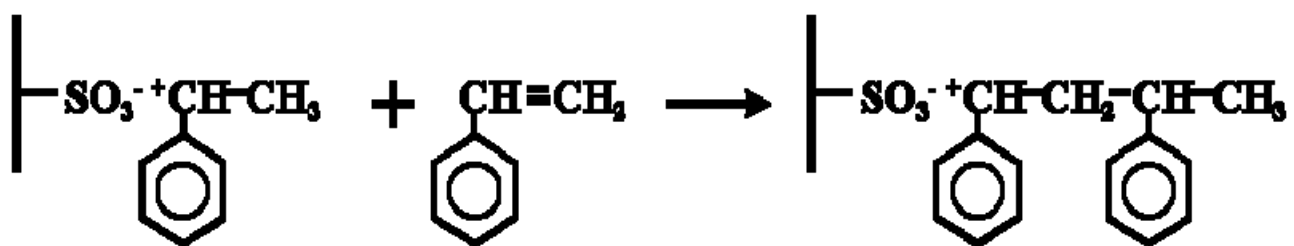


Figure 2-4. Propagation step for cationic polymerization of styrene.

In this work styrene and substituted styrene monomers will be used to form polymer grafts. Styrene proceeds by cationic polymerization through electrophilic addition to the growing carbocation and the phenyl ring stabilizes the newly developed cation [103-106]. PES has been sulfonated using sulfuric acid to impart hydrophilicity [107-108]. Styrene monomer undergoes polymerization reaction and polymer grafts are formed in the pores of membrane (Figure 2-5).

This research work deals with creation and understanding of polymeric functionalized membranes by sequential cationic polymerization of styrene and substituted styrene monomers (CMS and ES). A variety of functionalities (phenyl, sulfonic acid, chloromethyl, and ethoxy) have been incorporated for attaching the grafts. Homopolymer and block copolymers are formed in the pores of microfiltration membrane. These block copolymers will be the first step in creating a synthetic analog of ligands used in affinity chromatography for antibody separation.

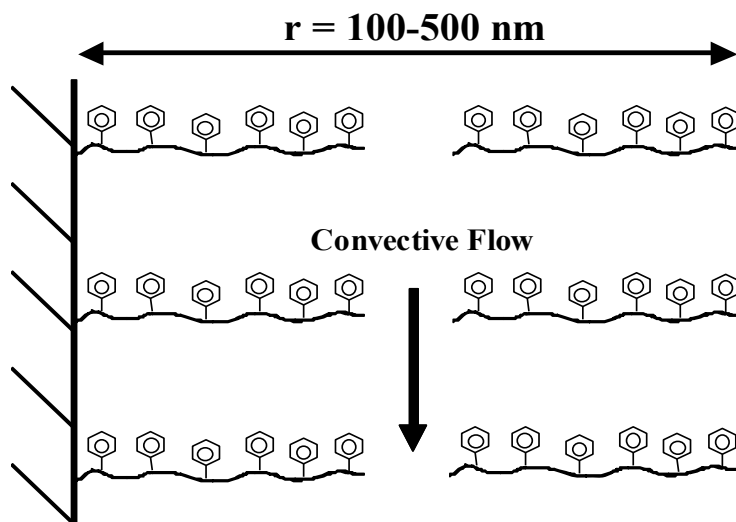


Figure 2-5. Polystyrene grafts in a membrane pore.

CHAPTER 3 EXPERIMENTAL PROCEDURE

3.1 Introduction

Functionalized membranes in this work were prepared by a three step procedure. These steps include sulfonation of the raw membrane, polymerization of styrene in the pores of the sulfonated membrane, and polymerization of chloromethylstyrene or 4-ethoxystyrene to create a block copolymer of styrene/chloromethylstyrene or styrene/4-ethoxystyrene, respectively. In this chapter, the material, instruments used for analytical studies, calibration methods, and procedures for immobilizing the initiator and formation of the block copolymer (styrene/chloromethylstyrene and styrene/4-ethoxystyrene) grafts are described.

3.2 Materials

Commercially available PES membranes were obtained from Millipore Corporation, Bedford, MA (Catalogue #GPWP04700). Membrane properties include an average pore size of 0.22 μm , a thickness of 165 μm , and a diameter of 47 mm. The chemical structure of polyethersulfone is given in Figure 3-1.

Sulfuric acid solutions of 0.5N were prepared from 99% sulfuric acid and distilled water. Base solutions of 0.1N sodium hydroxide were prepared from 1N sodium hydroxide solution by dilution. Styrene, chloromethylstyrene (CMS) and 4-ethoxystyrene (ES) were used for polymerization and formation of block copolymers.

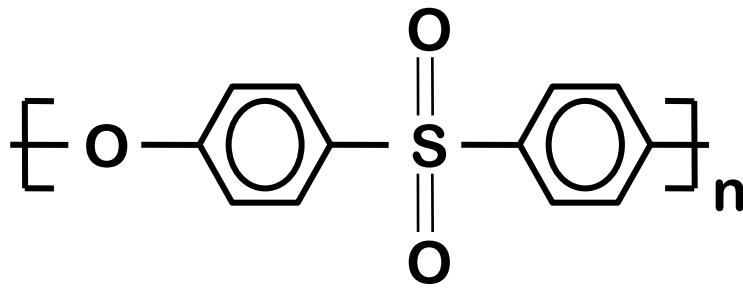


Figure 3-1. Repeat unit structure of polyethersulfone.

All the monomers were stored at 5°C until needed. Laboratory grade toluene was used as a solvent since it is soluble with styrene, ES and CMS. Laboratory grade methanol served as the sample diluter for analysis of styrene-toluene and chloromethylstyrene-toluene permeates by UV-Visible spectroscopy. Methanol was also used as sample diluter for ES-toluene permeate solution for gas chromatography analysis. All chemicals and solvents were obtained from Fisher Scientific (Pittsburgh, PA) and VWR (West Chester, PA) unless otherwise stated. The solvents were used as received without further purification except where noted.

3.3 Methods

The membranes used in this research are prepared by a simple, three step procedure. Initiator for the polymerization is immobilized in the membrane, a solution of styrene in toluene is permeated to create a homopolymer brush structure, followed by permeation of CMS or ES to form diblock copolymer brush. Figure 3-2 shows the schematic of the experimental laboratory setup. The first step is to wash the whole apparatus with distilled water. This is done by flushing distilled water from the top of the tank and allowing the water to flow through the membrane holder by keeping the valves (upstream and downstream of membrane holder) open. The pH of the water collected from bottom is checked and the apparatus is washed until the pH reaches 7. The microfiltration (220 nm pore size) membrane, in the form of white circular (47 mm diameter) disc, is kept in a versatile stainless steel membrane holder. The valves upstream and downstream of membrane holder are closed and the reaction solutions are fed into the carbon steel feed cell. The feed tank is then pressurized with pure nitrogen (zero grade to prevent contamination) at 21 psig and kept constant with the help of a regulator on the nitrogen cylinder. The tank pressure is indicated by a pressure gauge attached at the top of the tank.

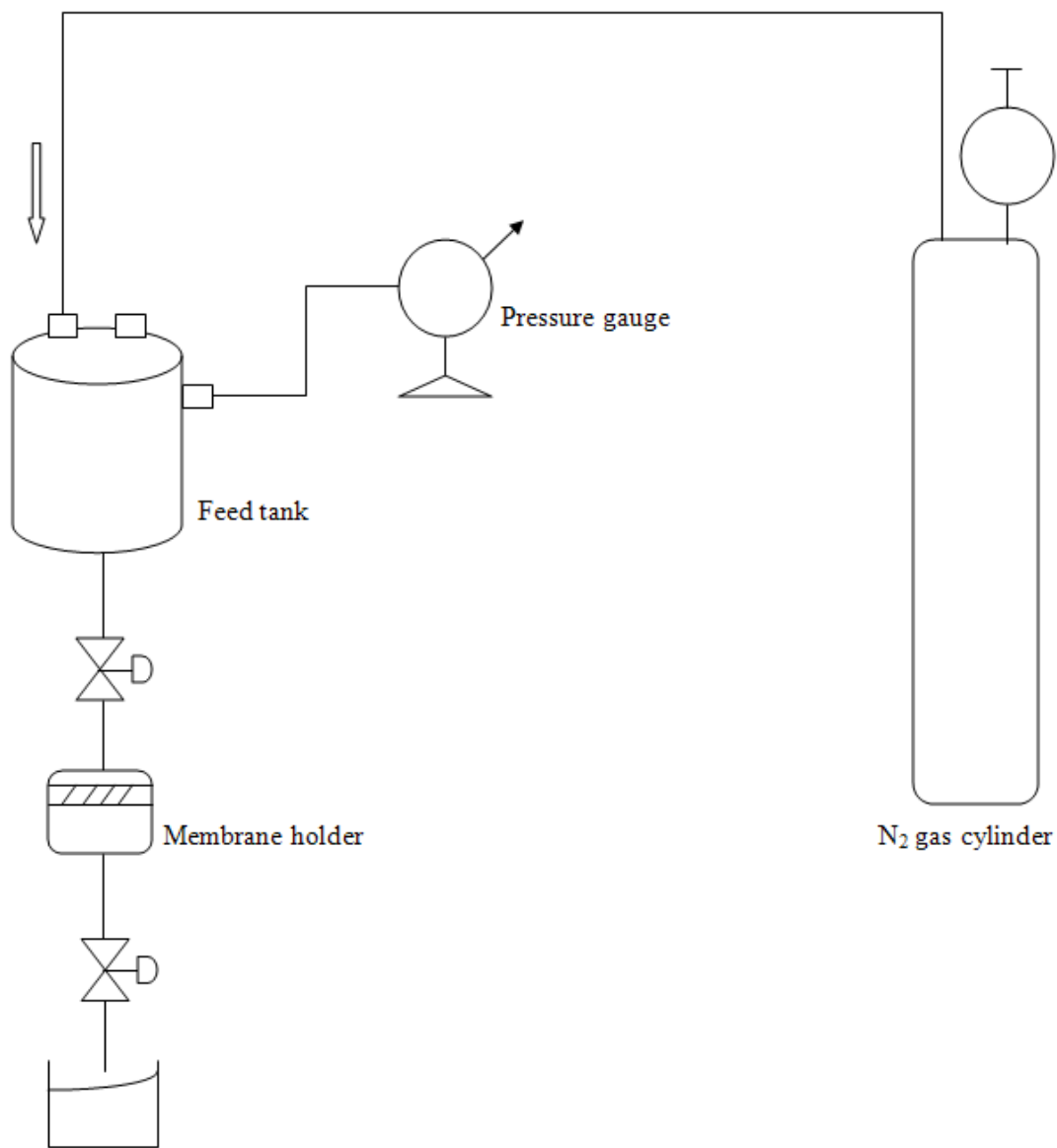


Figure 3-2. Schematic of the experimental laboratory setup.

Next, the valves are opened to allow the reaction solutions to permeate through the membrane. Permeate is collected at atmospheric pressure from the bottom. All experiments were performed at room temperature. It should be noted that, since the membrane is microfiltration with large pore size, the flow rate of solution through the membrane is very high. Hence, a valve downstream of membrane holder was kept half open to maintain a flow of 1 ml/min. Additionally, pure water flux can be measured after each stage of modification to determine permeability.

3.3.1 Initiator immobilization

The feed tank is filled with 250 ml of 0.5N H₂SO₄ and sulfuric acid is allowed to permeate through the membrane for 3 hours. After permeation of sulfuric acid the membrane is taken out of the membrane holder and rinsed multiple times with distilled water until the pH of the washed water reaches 7. The membrane is then allowed to dry in air (~2 hours) until the mass is constant. The apparatus is washed with distilled water after acid treatment and allowed to dry.

3.3.2 Synthesis of homopolymer brush

Styrene, ES and CMS monomers were used to create homopolymer brushes by treating the sulfonated membrane with the desired monomer. The sulfonated membrane was wetted with pure toluene for a few seconds and immediately placed on the membrane holder prior to the polymerization step to prevent membrane cracking. In all cases, a 5 vol% of monomer in toluene (100 ml of Styrene/CMS-toluene and 25 ml of ES-toluene) solution is permeated at constant pressure drop of 21 psi across the membrane for 120 minutes. The permeate is collected from the bottom and the volume is measured. The membrane is then washed with pure toluene by permeating toluene through the membrane to remove the unreacted styrene. Unreacted styrene in

the washed toluene is measured by UV-Visible spectroscopy at the characteristic peak wavelength of 291 nm using methanol as solvent.

3.3.3 Synthesis of block copolymer brush in the membrane matrix

Block copolymers are formed by polymerization of styrene, followed by polymerization with CMS or ES to create grafts of poly(styrene-co-CMS) or poly(styrene-co-ES), respectively. After styrene polymerization, the feed tank was washed thoroughly with toluene to remove residual styrene (~2 washes). Next, the block copolymer was formed by permeating 5 vol% of 100 ml CMS/toluene or 5 vol% of 25 ml ES/toluene through polymerized membrane at a constant pressure drop of 21 psi. The permeation is continued for 120 minutes. The permeate is collected and the volume is measured. The membrane is allowed to dry in air and the mass of the membrane is measured.

3.3.4 Membrane permeability

The feed tank, membrane holder and connecting pipes, as shown in Figure 3-2 are rinsed with distilled water. The feed tank is next filled with distilled water. The membrane is placed into the membrane holder. The valves upstream and downstream of membrane holder are closed. The tank is then pressurized by adjusting the pressure to 5 psig using the pressure regulator on the nitrogen cylinder. The valves are then opened and the system is allowed to come to steady state (~ 5 minutes) until the flow rate is constant. The permeate is collected at 2 minutes intervals and three readings are taken. The process is repeated with a full tank and at incremental pressures of 10, 15, 20, 25 and 30 psig.

3.4 Analysis

3.4.1 Ion-exchange capacity (IEC)

The ion-exchange capacities of the raw and functionalized membranes were quantified by elemental analysis of regenerated sodium ions ($\lambda = 589 \text{ nm}$) in sulfuric acid solution using atomic absorption spectroscopy (Varian 220 FS). In each case, the membrane was treated with 0.1N NaOH (100 ml) by convection for approximately 180 minutes at a pressure drop of 21 psi. The membrane was then rinsed with deionized water to remove any non-specifically bound sodium in the membrane pores. Finally, the membrane was retreated with 0.5N H₂SO₄ (250 ml) for 180 minutes to regenerate sodium ions from the pores. Figure 3-3 illustrates the standard calibration curve prepared by dilution of a 2 mg/l of Na⁺ (reference standard 1 mg/ml) ions in deionized water. Ion-exchange capacity is calculated as total milliequivalents of sodium ions available for exchange per gram dry weight of sulfonated membrane. The amount of sodium recovered is used to determine the number of available sulfonic acid groups in the membrane.

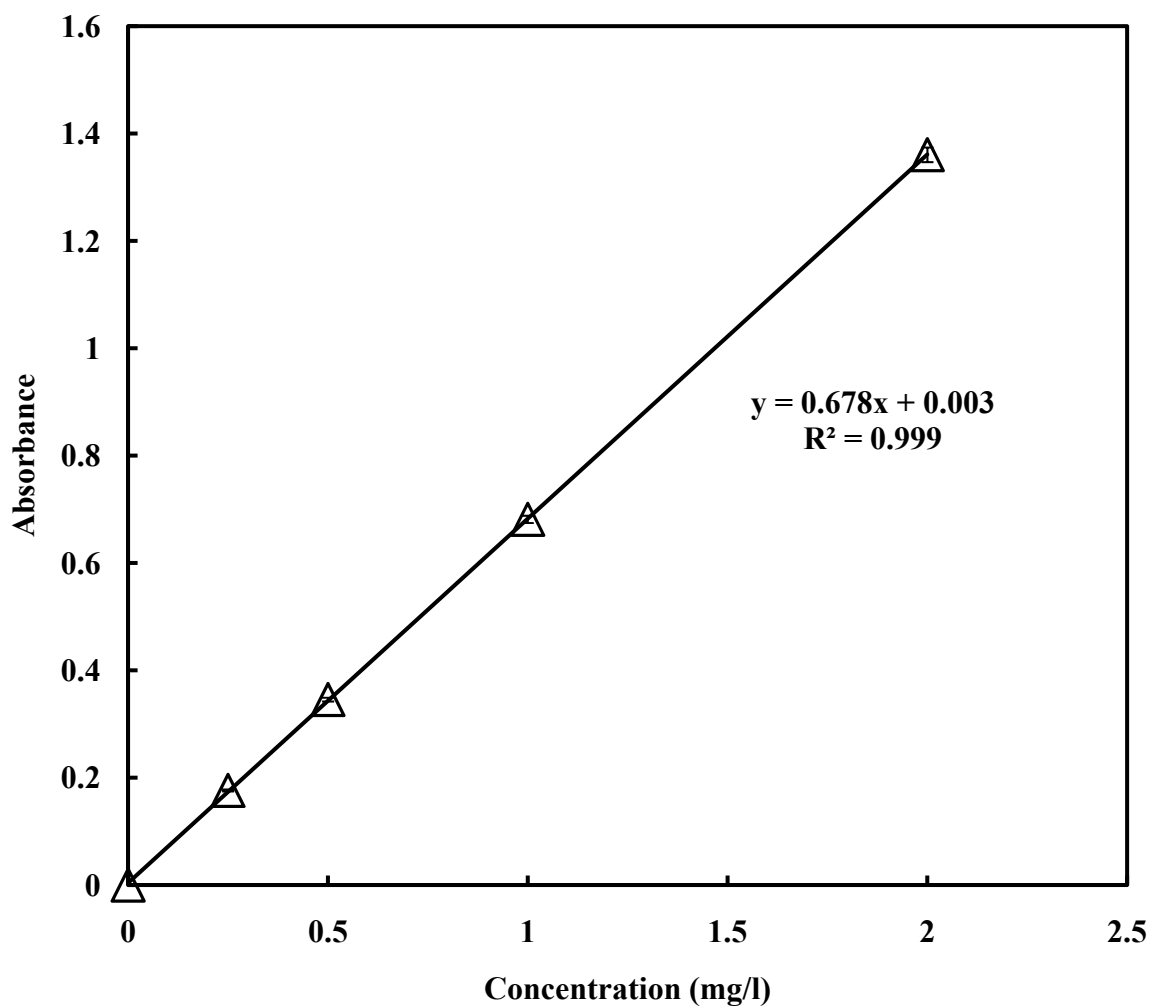
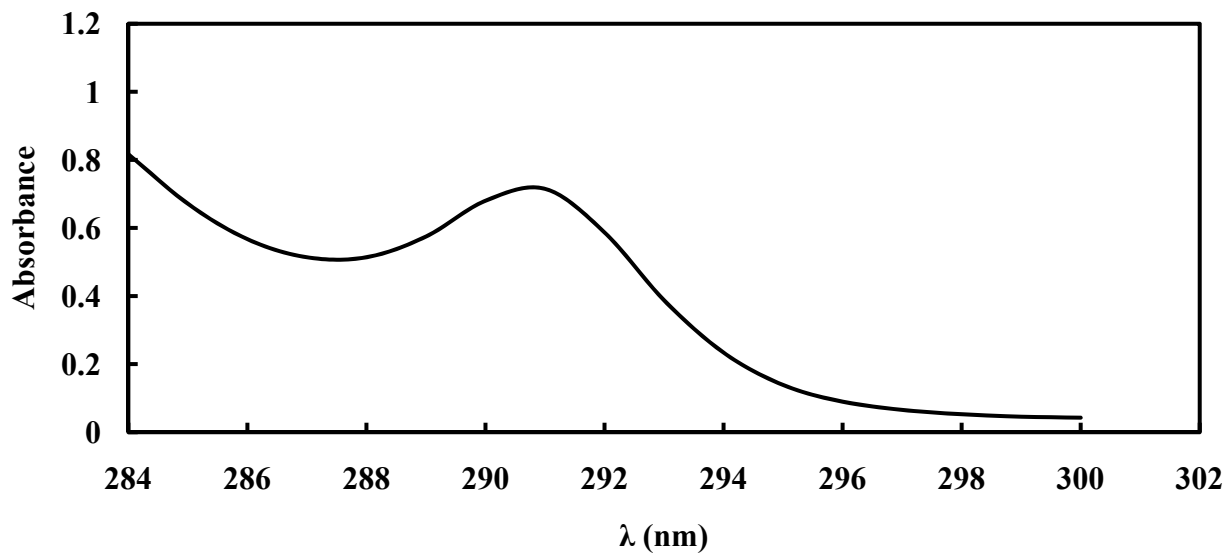


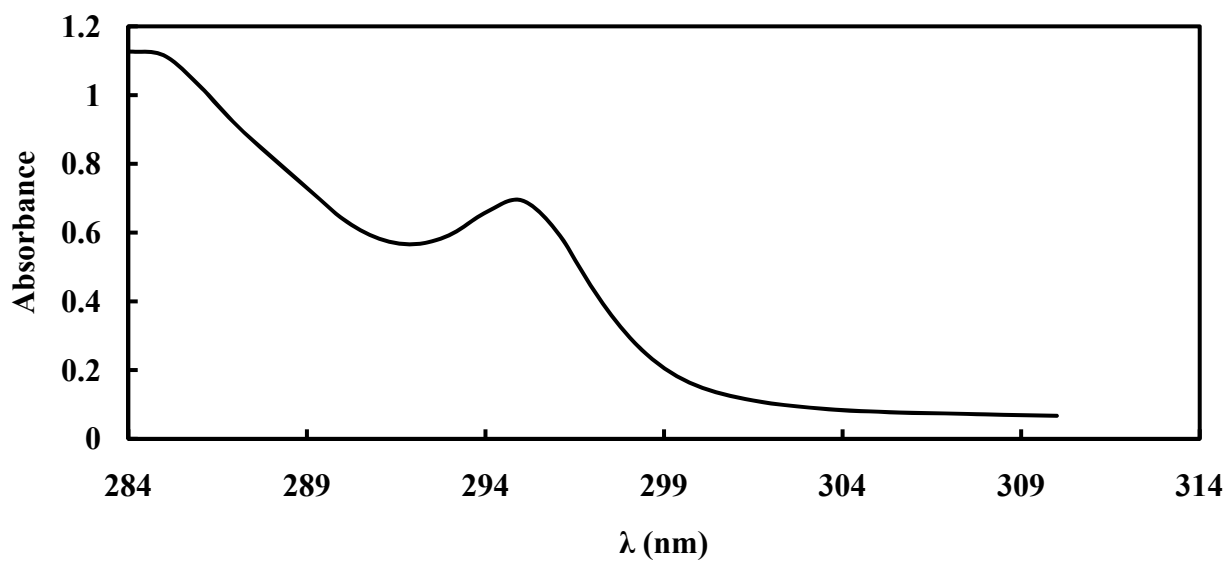
Figure 3-3. Standard calibration curve for IEC analysis by atomic absorption spectroscopy using sodium ion ($\lambda = 589$ nm).

3.4.2 UV-Visible spectroscopy analysis

Samples of styrene-toluene and styrene-CMS were diluted 1:1250 and 1:416, respectively, with pure methanol. Styrene and CMS monomer concentrations were quantified in the feed and permeate samples after polymerization by UV-Visible spectrophotometry at characteristic peak wavelengths of 291 and 295 nm, respectively (Figure 3-4). The characteristic peak wavelength of toluene is at 281 nm (Figure 3-5), so there was no interference. Spectral data was obtained using a Shimadzu UV-2401 spectrophotometer. The standard calibration curves for styrene (Figure 3-6) and CMS were obtained by analysis of different concentrations in the photometric mode.



(a)



(b)

Figure 3-4. UV-spectrum of (a) pure styrene showing characteristic peak at 291 nm, and (b) UV-spectrum of pure CMS showing characteristic peak at 295 nm.

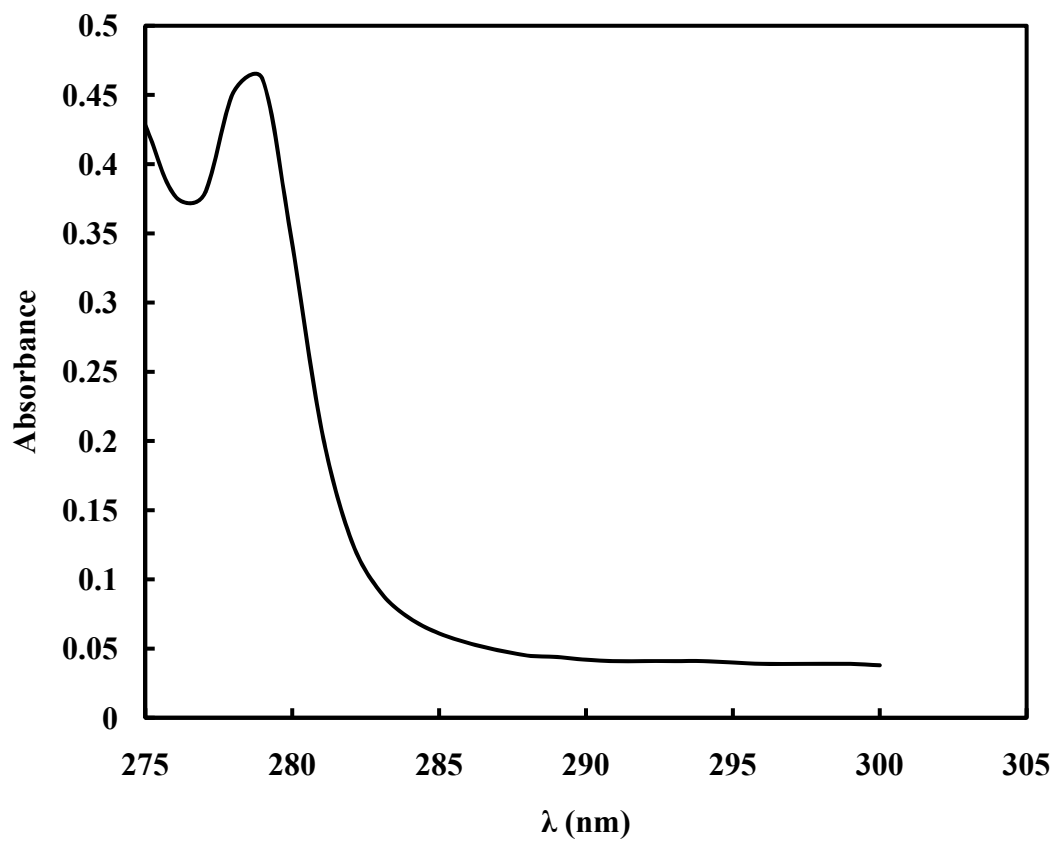


Figure 3-5. UV-spectrum of pure toluene showing characteristic peak at 281 nm.

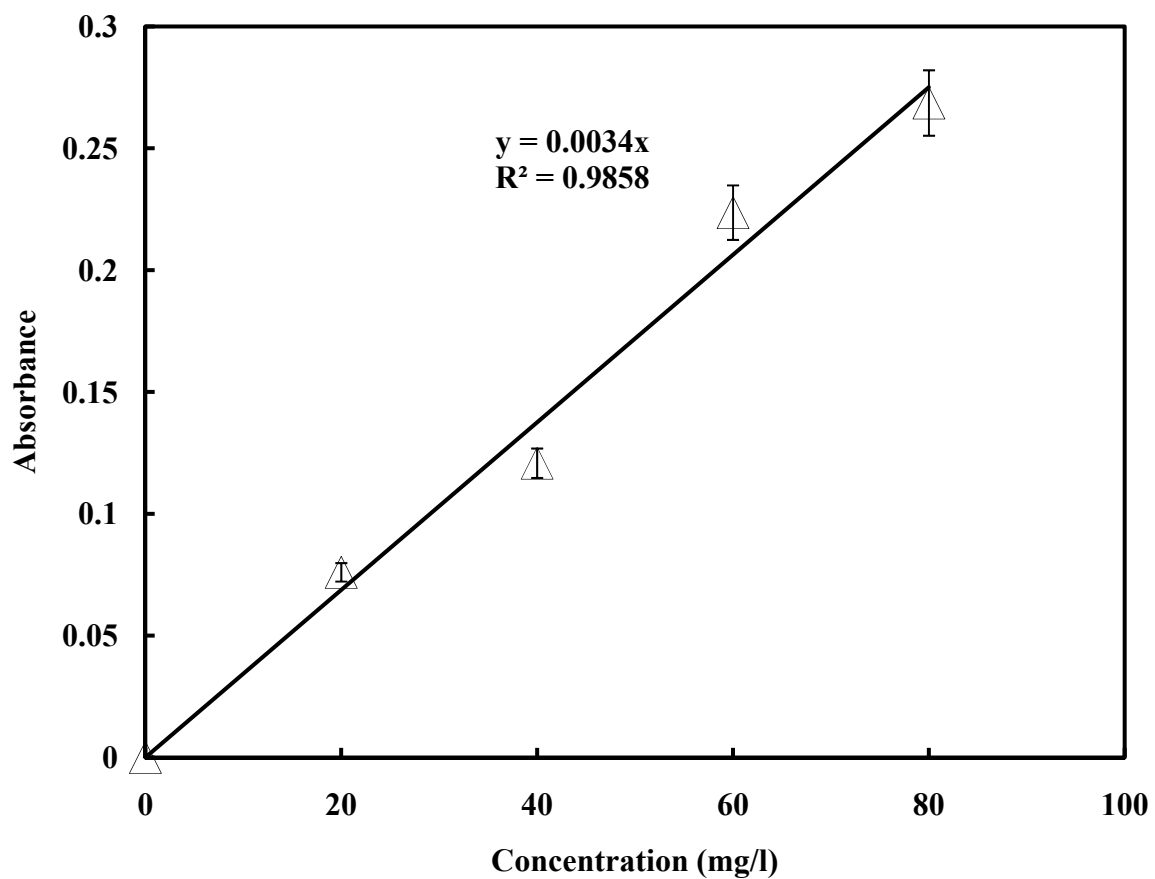


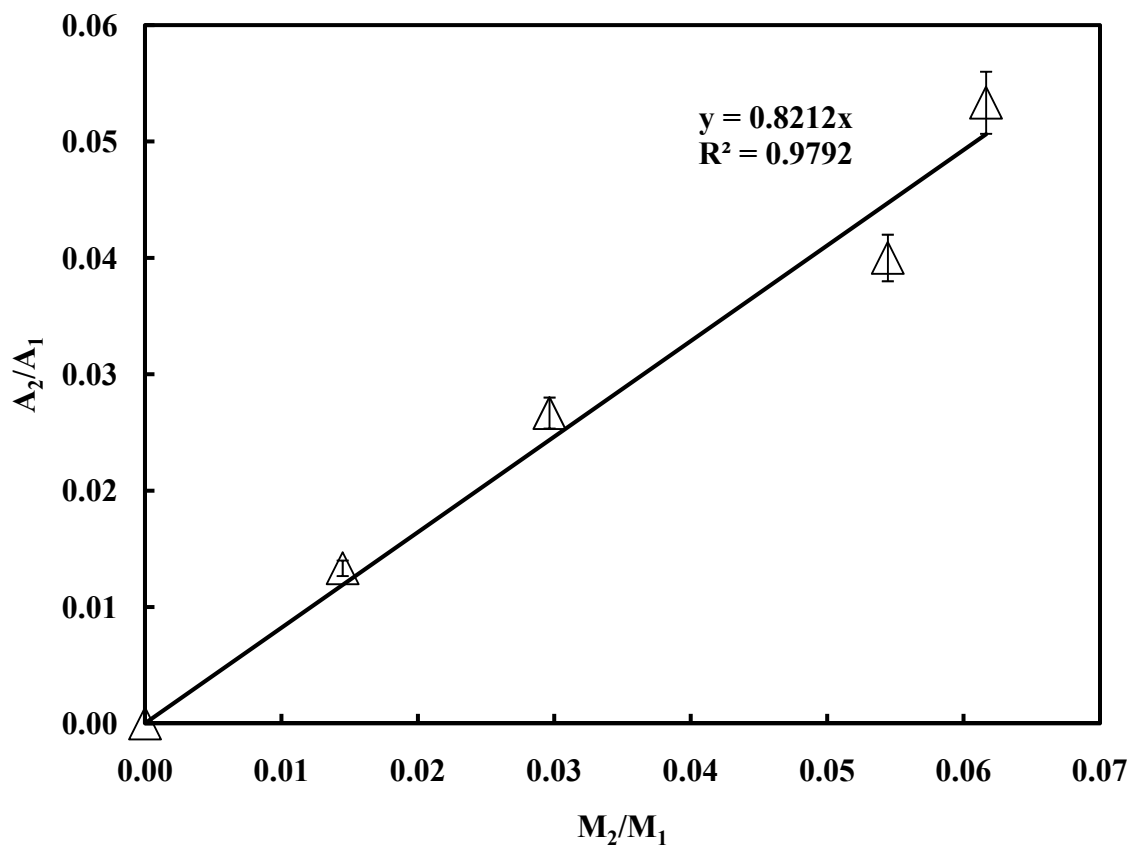
Figure 3-6. Standard calibration curve for styrene analysis at 291 nm by UV-spectrophotometry.

3.4.3 Gas chromatography analysis

Samples of ES-toluene were diluted 1:1 with pure methanol. ES concentrations were determined in the feed and permeate solutions using gas chromatography at its elution time of 1.56 minutes. The elution times of methanol and toluene are 0.1 and 0.2 minutes, respectively, so there was no interference. All reaction samples were analyzed using a Shimadzu GC-14A gas chromatograph equipped with a flame ionization detector. A 30m X 0.53mm i.d capillary column (Rtx-624, Restek Corporation) containing a 6% cyanopropylphenyl and 94% dimethyl polysiloxane based stationary phase was used for analysis. The gas chromatograph parameters are shown in Table 3-1. Helium was used as the carrier gas. Hydrogen and compressed air gases were used to ignite the flame. The GC range was kept at 3 in order to avoid flat top peaks and get good resolution. Figure 3-7 illustrates the standard calibration curve for ES obtained by analysis of different concentrations. The results from the extensive experiments carried out to synthesize and characterize these functionalized membranes will be discussed in the next chapter.

Table 3-1: Gas chromatograph column parameters.

Parameter	Value
Helium pressure (kPa)	470
Hydrogen pressure (kPa)	110
Air pressure (kPa)	120
Oven temperature (°C)	125
Run time (min)	5
Range	3



A_2 - Area under the curve for ES

A_1 - Total area under the curve for toluene and methanol

M_2 - % Concentration of ES

M_1 - % Concentration of toluene and methanol

Figure 3-7. Standard calibration curve for ES analysis by gas chromatography.

CHAPTER 4

RESULTS AND DISCUSSION

4.1 Introduction

This chapter contains detailed results and discussion involved in the synthesis of multiple adsorptive sites immobilized in the pores of a microfiltration membrane. Modifications to the functionalized membrane have been quantified at each stage. Functionalized membranes were studied in terms of synthesis and quantification of initiator immobilization and polymerization reactions. This includes formation of homopolymer and block copolymer grafts, and determination of ion-exchange capacity, average graft length and membrane permeability. Furthermore, influences of initiator contact time and monomer feed concentration on polymer growth have been studied. These membranes have high dynamic and equilibrium binding capacity, and are expected to be effective for large scale purification of MAbs.

4.2 Membrane permeability studies

Permeability studies were carried out in a batch mode. A flat sheet membrane disc made from polyethersulfone was used in all experiments. The PES membranes were sealed with a 4.1 cm inner diameter o-ring. Therefore, 4.1 cm was considered as the membrane effective diameter for calculating the flux. The membrane effective area was 13.2 cm^2 . Pure water permeation flux is directly proportional to pressure drop, and the slope of the straight line gives the membrane permeability.

Permeability studies were carried out on raw, sulfonated, styrene grafted and styrene-co-CMS grafted membranes to compare the effects of polymer graft formation on membrane flux. Polymer growth in the pores of the membrane should reduce the effective pore size in each case,

and therefore a decrease in permeability was expected. Figure 4-1 illustrates the effect of each treatment on water flux of the membrane. The permeability of raw membrane was computed to be 1.98 ml/cm²/min/psi. The permeability decreased by 58% after sulfonation. An increase in SO₃⁻H⁺ group density decreased the permeability of the pure water. This is most likely due to the sulfonation reaction forming hydrogel in the pores that would constrict the membrane pores thereby reducing the effective pore size. SEM micrographs confirming formation of hydrogels due to sulfonation of aryloxy or arylamino groups linked to polymers like phosphazenes have been reported [113].

Sulfonation was followed by polymerization of styrene which resulted in further reduction of the permeability by 3.3 times. This is because polystyrene grafts were formed in the membrane flow path, reduced the effective pore size, and consequently decreased the permeability. Styrene polymerization was followed by CMS polymerization. The decrease in permeability in this case was 2.7 times as compared to the styrene grafted membrane. This is because the longer polymer grafts increased resistance to flow. The results are consistent with results reported by other researchers where they have observed a drop in permeability after functionalization showing evidence of polymer grafting [101, 109, 114]. It should be noted that the permeability of styrene-co-CMS grafted membrane was 0.09 ml/cm²/min/psi which is higher than the permeability of a 300 kDa MWCO PES UF membrane (0.019 ml/cm²/min/psi) based on the manufacturer reported test criteria. Therefore, although the pore size is reduced, these materials are still microfiltration membranes and are not plugged by formation of polymer grafts. Large molecules, such as IgGs (MWCO 100-150 kDa), can be expected to be transported through the membrane by convection.

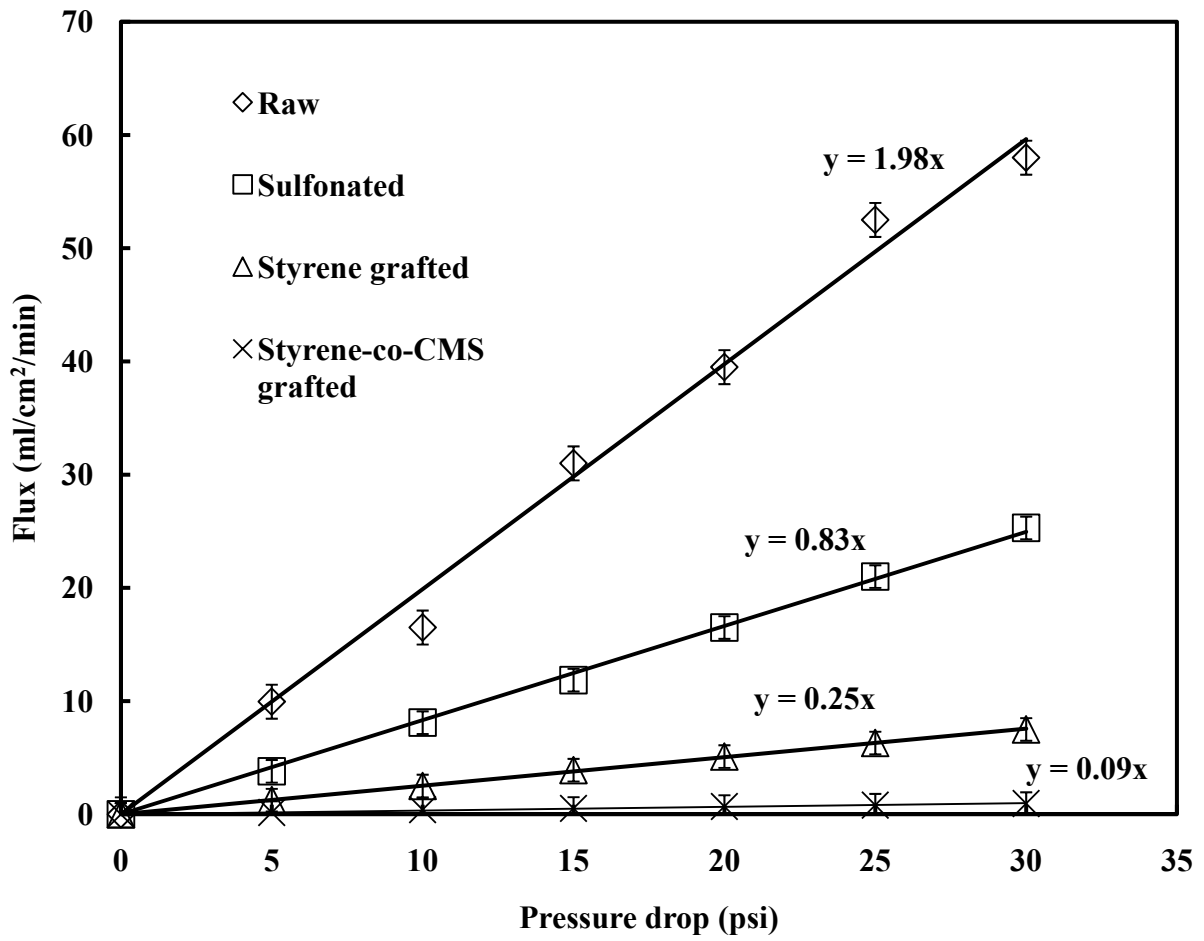


Figure 4-1. Polymer growth effect on membrane permeability.

4.3 Quantification of membrane sulfonation

The raw PES membrane was sulfonated to immobilize sulfonic acid groups as initiator for cationic polymerization. The sulfonic acid concentration was quantified by ion-exchange studies. Ion-exchange capacity (IEC) is the parameter that quantifies the number of ionizable groups in the membrane. IEC was determined in terms of milliequivalents of sodium ion exchanged per gram of membrane (dry weight).

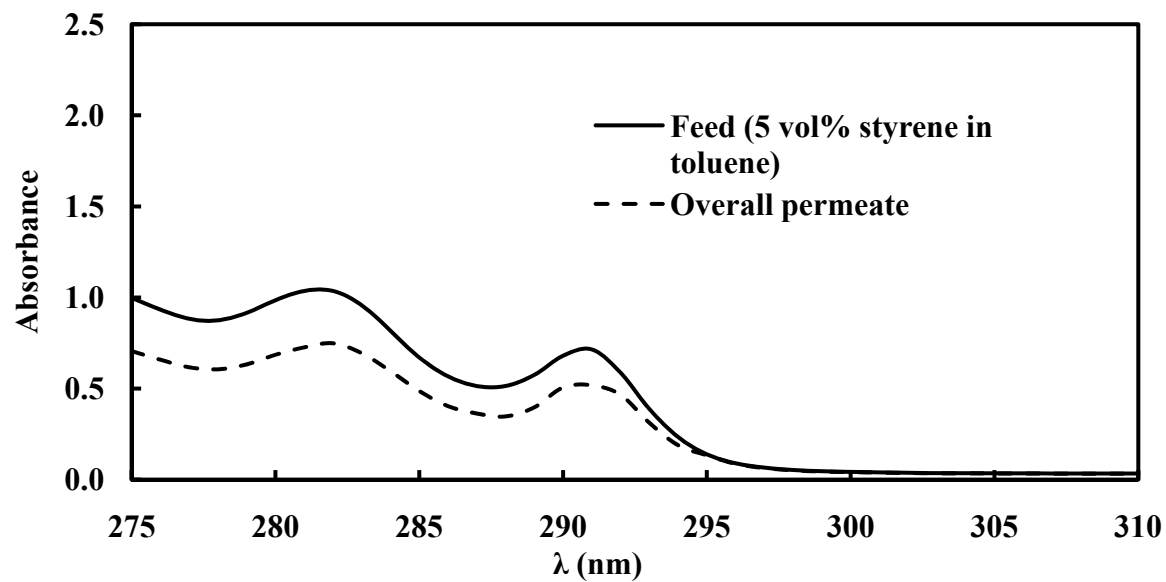
The IEC of the raw membrane was determined experimentally to be 0.013 meq/g dry membrane. Ionizable groups are present due to mild surface modification performed by the manufacturer to improve membrane hydrophilicity. Sulfonated polyethersulfone membrane has a maximum theoretical ion-exchange capacity of 0.32 meq/g. This value is based on an average pore size of 0.22 μm and 70% membrane porosity, yielding a total internal surface area of 30.75 m^2/g based on parallel, cylindrical pores with length equal to membrane thickness [110]. The IEC of the sulfonated membrane was experimentally determined to be 0.15 meq/g. This represents 46% of the maximum theoretical IEC. The higher IEC of the sulfonated membrane relative to the raw membrane was attributed to immobilized sulfonate groups in the membrane. The raw membrane represented less than 5% of the IEC of the sulfonated membrane. In addition, the internal surface area was >99.9% of the total membrane area, and therefore sulfonate groups are mostly in the pores of the membrane and not on the external surface area. The results are consistent with work done by Ritchie and coworkers who demonstrated successful introduction of sulfonic acid group onto PES. FTIR was used to characterize membrane sulfonation. Comparison of spectra of raw and sulfonated membrane showed the asymmetrical C-S bond stretching vibrations of sulfonic acid groups at wavenumber 950 cm^{-1} [109-110].

4.4 Synthesis and quantification of homopolymer brushes

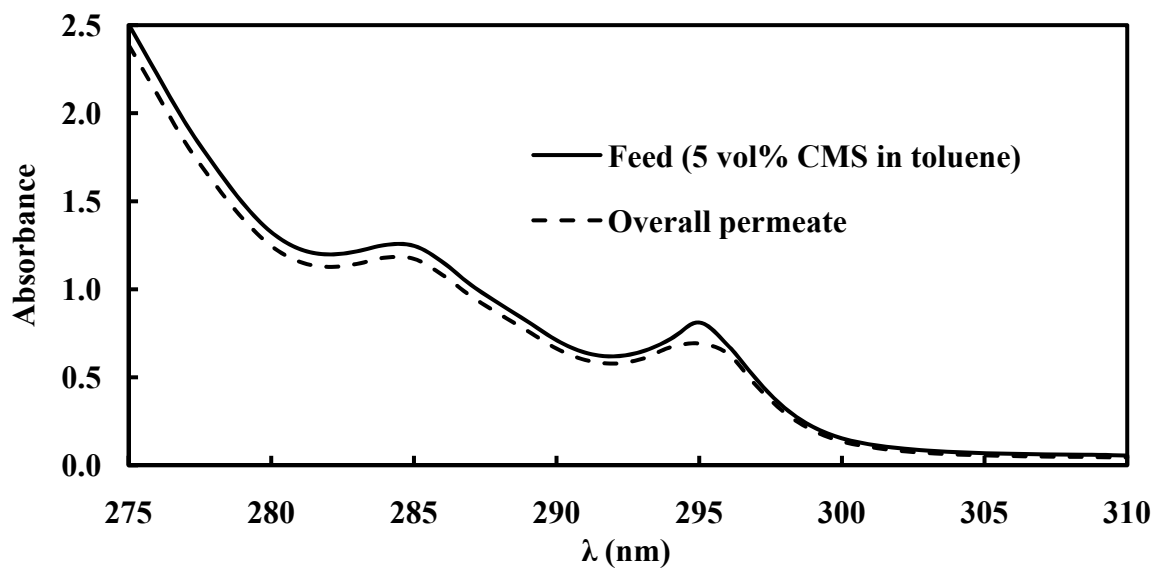
Styrene and the substituted styrene monomers CMS and ES were used for the formation of homopolymer brushes. In all cases, a 5 vol% feed solution of each monomer was used for polymerization of the sulfonated membrane. Initiator contact time was 180 minutes and polymerization reaction time was 120 minutes. Synthesis and quantification of each homopolymer brush confirmed that grafts with different functional groups (phenyl, ethoxy, chloromethyl) could be attached to the PES backbone.

4.4.1 Styrene and CMS graft quantification by UV-Visible spectroscopy

Decreases in styrene and CMS concentrations, and thus retention in the membrane, were observed and quantified by decreases in the absorbance at the characteristic peaks of 291 and 295 nm, respectively, by UV-Visible spectroscopy (UV-Vis). Figure 4-2 illustrates a representative absorbance scan of feed and permeate solutions for each monomer. It was observed that approximately 0.65 mmol of styrene and 0.4 mmol of CMS were retained on the membrane. Negligible decreases in absorbance were observed for either monomer when permeated through the raw membrane. This confirms that there was no graft formation in the pores of the membrane by cationic polymerization in the absence of initiator sulfonic acid groups. Additionally, when permeate samples were diluted in methanol to perform UV analysis no precipitation or cloudiness was observed. This confirmed that the polystyrene did not come out and was retained in the pores of membrane.



(a)



(b)

Figure 4-2. UV-VIS spectrum for quantification of (a) styrene disappearance, and (b) CMS disappearance.

4.4.2 4-Ethoxystyrene graft quantification by gas chromatography

The characteristic peak for ES (dilution factor 1:625) by UV-Vis was observed to be 283 nm. This was very close to the characteristic peak for toluene (dilution factor 1:1250) at 281 nm, and therefore some amount of overlapping was seen on the spectrum (Figure 4-3). However, gas chromatography showed very clear and distinct separation between peaks for ES, toluene and methanol (Figure 4-4). Consequently, the decrease in ES permeate concentration was quantified using gas chromatography at an elution time of 1.56 minutes which is far from methanol (0.1 minutes) and toluene (0.2 minutes). The calibration curve illustrated in Figure 3-8 was used to determine the concentrations of ES in the feed and permeate. It was observed that 0.52 mmol of ES was retained on the membrane.

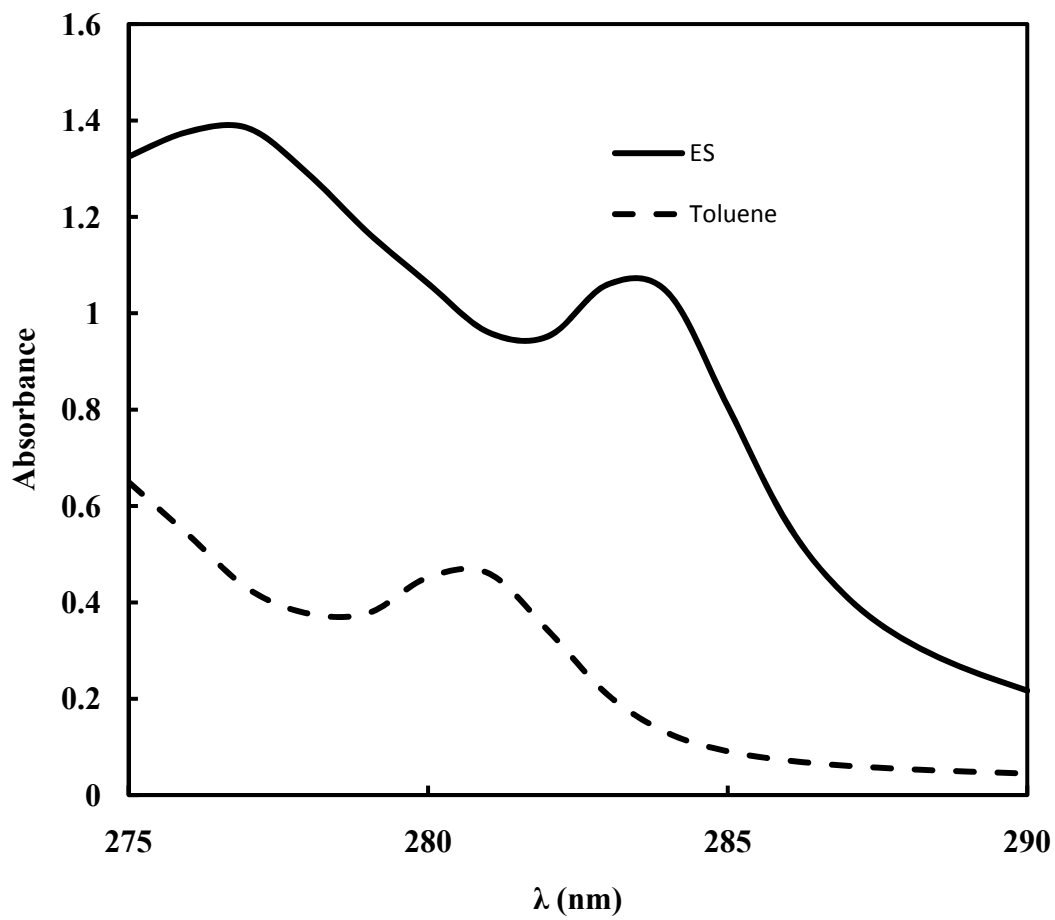


Figure 4-3. UV-spectrum of 4-ethoxystyrene and toluene showing characteristic peaks at 283 and 281 nm, respectively.

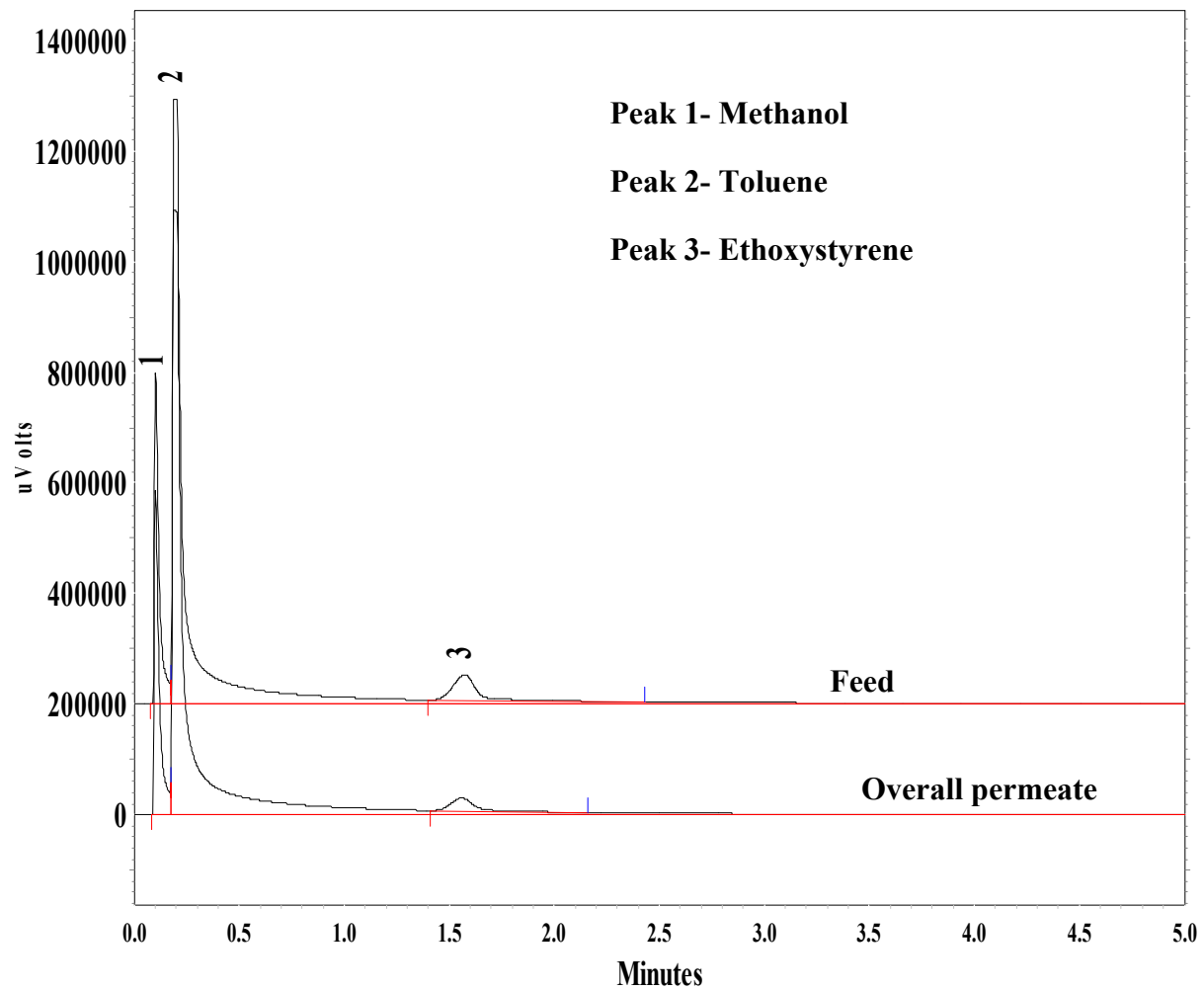


Figure 4-4. Gas chromatogram for quantification of ES disappearance.

4.4.3 Kinetics of each monomer reacted

The amount of monomer retained on the membrane was measured at definite intervals of time over 120 minutes. The membrane volume was calculated to be 0.21 ml based on an effective diameter of 4.1 cm and a thickness of 160 μm . Concentration was measured in terms of mmol of styrene reacted per ml of membrane. Concentration was plotted versus time as shown in Figure 4-5. It was observed that reaction of monomer was initially rapid and then gradually slowed down. This is most likely due to initial availability of active sites for polymerization. The growing grafts form a diffusion barrier that gradually slows down the reaction rate.

The pseudo-first-order kinetic expression shown in Equation 4.1 was used to model the experimental data [111, 112]:

$$Q_t = Q_e(1 - e^{-kt}) \quad (4.1)$$

where Q_e and Q_t are the amounts of monomer retained on the membrane ($\text{mmol}\cdot\text{mL}^{-1}$) at equilibrium and at time t (min), and k (min^{-1}) is the pseudo-first-order rate constant. Q_e was treated as an adjustable parameter in the above expression. The value of Q_e was determined by performing regression analysis using the method of least squares to best fit the model with experimental data. The linearized form of Equation 4.1 is shown in Table 4-1. The values of the rate constant, k , were determined from the slope of the straight line obtained by plotting $\ln(Q_e - Q_t)$ versus t . The values of k , Q_e and correlation coefficients (R^2) are shown in Table 4-1.

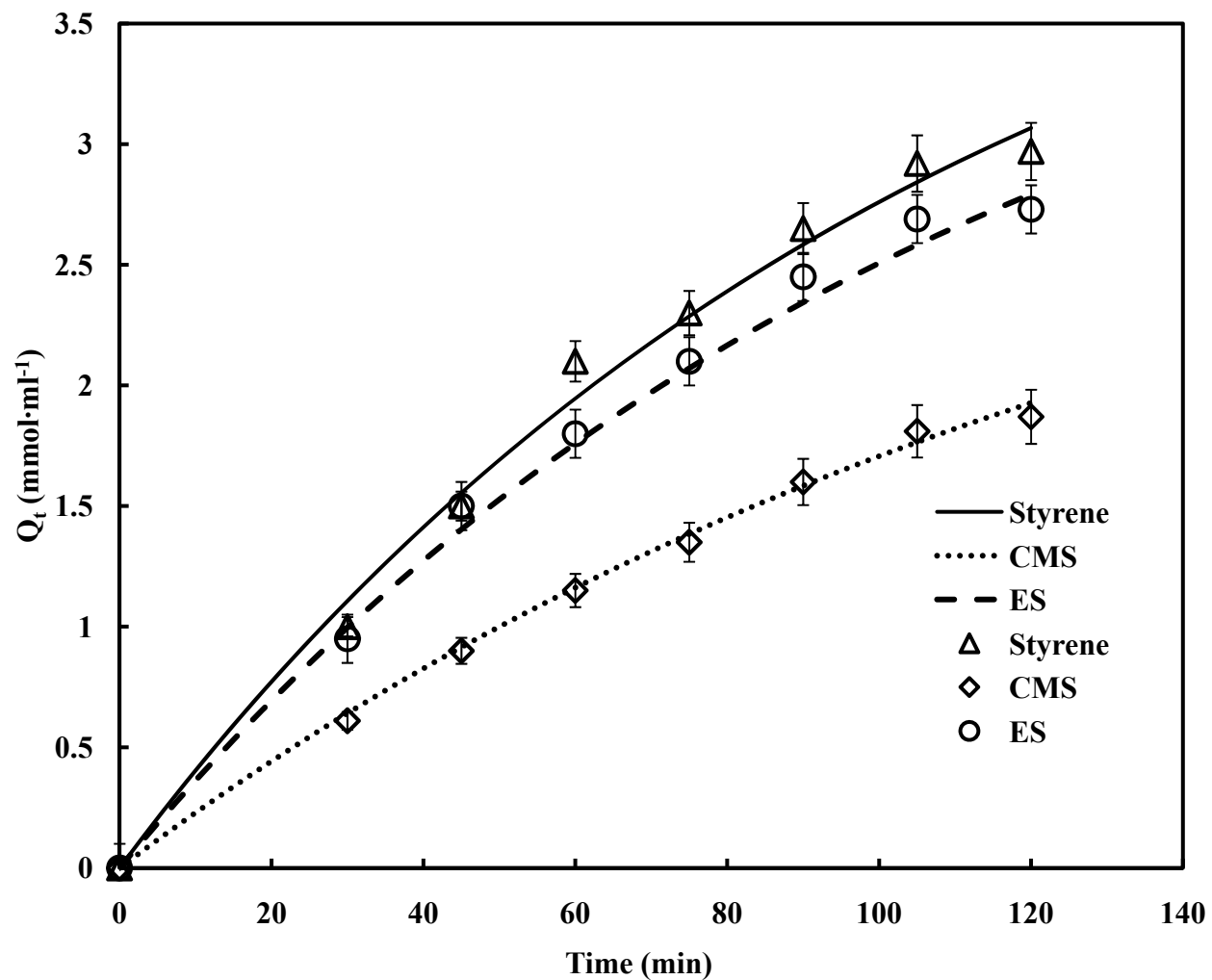


Figure 4-5. Kinetics of each monomer reacted. The smooth curves represent the pseudo-first-order equation fit and the data points represent experimental observations.

Table 4-1: Pseudo-first-order model parameters.
$$\ln(Q_e - Q_t) = \ln Q_e - kt$$

Monomer	k (min ⁻¹)	Q _e (mmol·ml ⁻¹)	R ²
Homopolymers			
Styrene	0.0092	4.6	0.9883
ES	0.0088	4.3	0.9914
CMS	0.0069	3.4	0.9974
Block copolymers			
Poly (styrene-co-CMS)	0.0059	2.2	0.9968
Poly (styrene-co-ES)	0.0075	3.8	0.9929
Different monomer feed concentration			
5 vol% styrene	0.0092	4.6	0.9883
10 vol% styrene	0.020	5.6	0.9613
15 vol% styrene	0.024	9	0.9721

It was observed from the R^2 values and Figure 4-5 that the model correlates well with the experimental data. By comparing the rate constants for different monomers it was observed that styrene and ES reacted approximately at the same rate while CMS reacted nearly 25% slower than styrene and ES. Furthermore, the slope between 100 and 120 minutes is still positive and not showing a plateau. This indicates that although the rate is gradually slowing down, the amount of monomer retained on membrane has not reached a maximum value and may increase if reaction is carried out beyond 120 minutes. This result is correlated with the model which shows a computed value of Q_e greater than predicted at 120 minutes of polymerization reaction time. Hence, the model holds well until 120 minutes of polymerization reaction time. However, the validity of the model needs to be investigated for reaction times beyond 120 minutes.

The amounts of monomer retained each for styrene, ES and CMS were 2.97, 2.73 and 1.87 $\text{mmol}\cdot\text{mL}^{-1}$, respectively, at 120 minutes of reaction time. This indicated that CMS is the least reactive and styrene and ES showed approximately similar reactivity. The low reactivity of CMS is due to the strong electron-withdrawing chloromethyl substituent. The presence of an electron-withdrawing substituent inhibits the reactivity of monomer because cationic polymerization is limited to electron-donor substituents. Alkoxy group is an electron donor, and therefore the higher reactivity of ES relative to CMS was reasonable. The results are consistent with those reported by Kamigaito and co-workers [115]. In their work, CMS showed low reactivity relative to styrene during homopolymerization and copolymerization by cationic polymerization using alcohol as an initiator and boron trifluoride etherate as an activator. Their work also showed that methoxy styrene was more reactive than CMS. This confirms that a monomer with an electron-donor group (alkoxy) is more reactive than a monomer with an electron-withdrawing group (chloromethyl).

4.5 Kinetics of CMS/ES during formation of block copolymer grafts

Figure 4-6 shows amounts of CMS and ES retained on the membrane after polymerization with styrene. The pseudo-first-order rate expression discussed in section 4.4.3 was used to model the experimental data. Correlation coefficients show reasonably good fits of the experimental data with the model. The values of k are reported in Table 4-1 and indicate that formation of styrene-co-ES block copolymer was roughly 1.25 times faster than styrene-co-CMS block copolymer. The amount of CMS and ES retained on the membrane during formation of block copolymer was 60 and 80%, respectively, of the amount retained during formation of homopolymer. This was most likely due to lower site accessibility because of the diffusion barrier caused by the already present styrene grafts.

4.6 Controlled polymer growth

4.6.1 Introduction

In this study, controlled growth of styrene polymer was evaluated through the variation of reaction parameters like monomer feed concentration and initiator reaction time. The study aimed to build an understanding of the process of polymer growth and the reaction mechanism so that data could be used in the future for further optimization of specific applications like antibody adsorption. The kinetics of polymer growth, average graft length, and IEC were evaluated as a function of these reaction parameters.

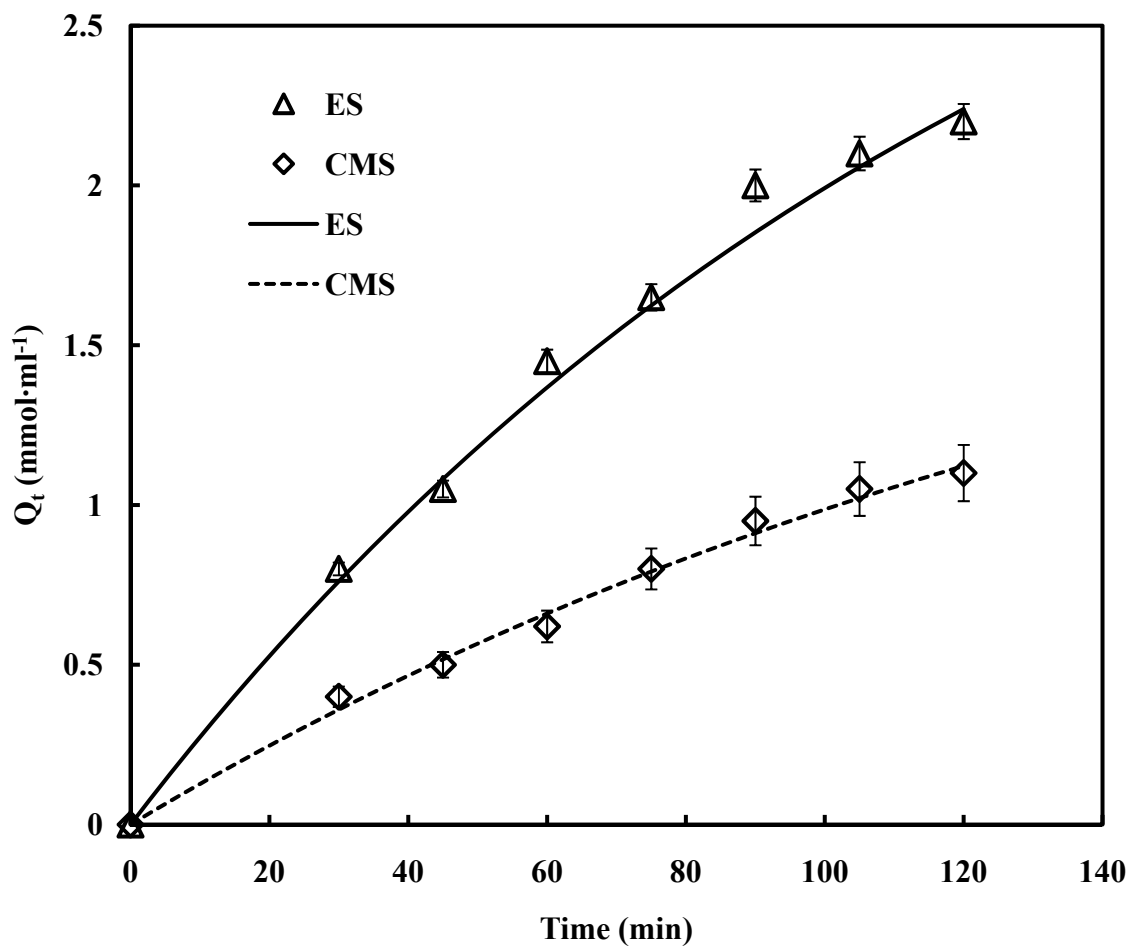


Figure 4-6. Kinetics of CMS and ES reacted after polymerization with styrene. The smooth curves represent the pseudo-first-order equation fits and the data points represent the experimental observation.

4.6.2 Influence of monomer concentration

4.6.2.1 Kinetics

Styrene reaction kinetics were studied for different feed concentrations. The plot of styrene retained versus time is shown in Figure 4-7. The pseudo-first-order rate expression (Equation 4.1) was used to fit the experimental data. The values of k , Q_e and R^2 were obtained by the same method as described in section 4.4.3, and are reported in Table 4-1. It can be observed that experimental data matches reasonably well with that predicted by model. The reaction proceeds rapidly and then gradually slows down. However, it should be noted that it did not show a plateau within 120 minutes of polymerization reaction time. It was observed from experimental data that the amount of monomer retained on membrane at 120 minutes of reaction time increases approximately linearly with monomer feed concentration. By comparing the value of rate constants it was observed that the rate of reaction for 15% monomer feed concentration was roughly 1.2 and 2.6 times higher than 10 and 5% feed concentration, respectively. Furthermore, it was observed that the value of Q_e almost doubled as the monomer feed concentration increased from 5 to 15%. This indicated that a higher feed monomer concentration increased the driving force for mass transfer through the grafts.

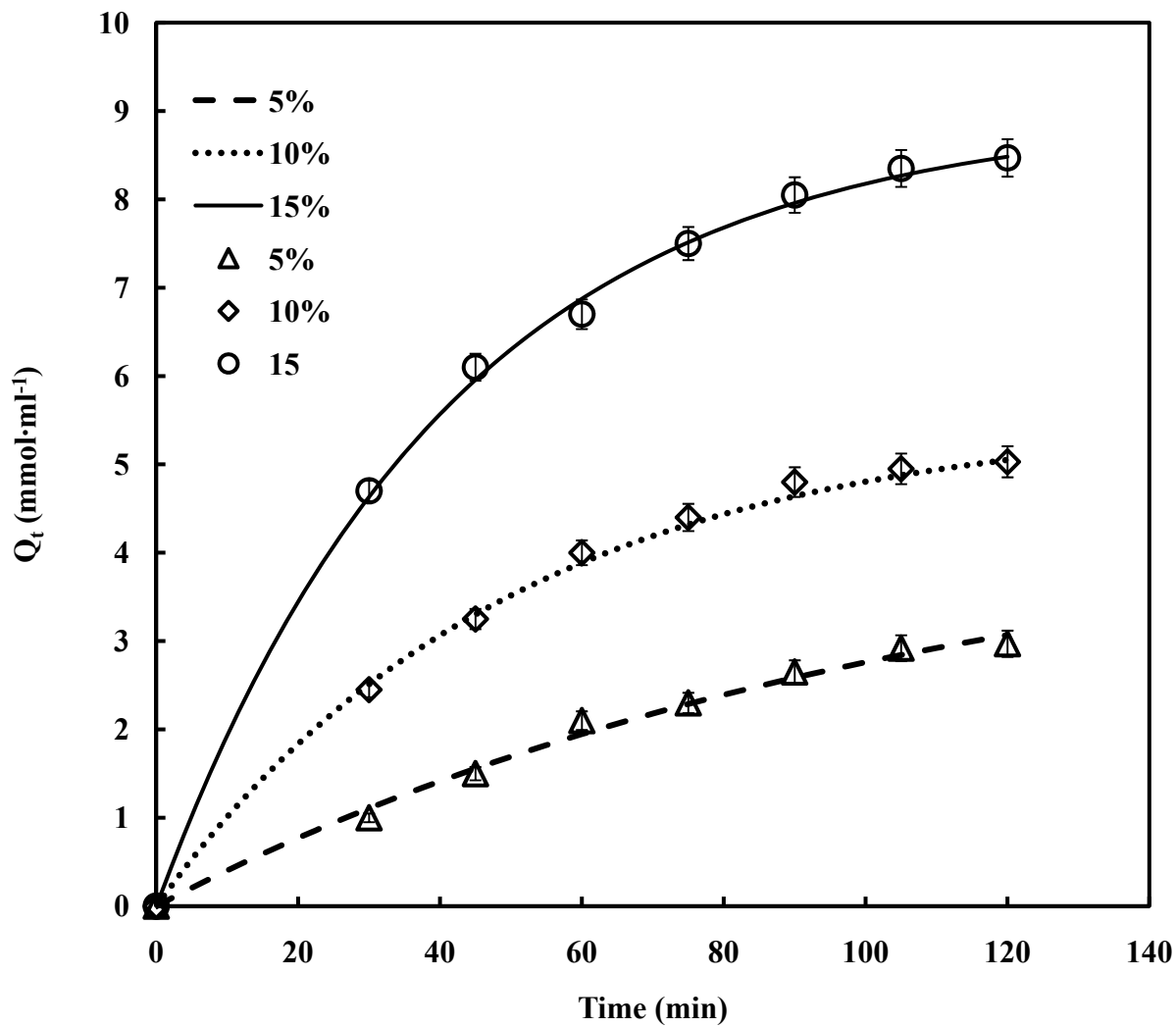


Figure 4-7. Kinetics of styrene reacted for different feed concentration. The smooth curves represent the fit with pseudo-first-order equation and the data points represent the experimental observation.

4.6.2.2 Graft length

Graft length as a function of monomer concentration was measured in terms of average number of repeat units per chain. It was calculated by determining the ratio of the number of styrene molecules reacted to the number of initiator sites. This determination assumed that all the styrene retained on membrane undergoes polymerization and that unreacted styrene remains in the permeate. The assumption was justified because reacted styrene becomes part of the carbocation that interacts with the immobilized initiator (sulfonic acid groups). Also there was no evidence of styrene monomer absorbed by the membrane. The bulk of the polymer grafts are formed in the membrane pores because the external surface area is 0.1% of total available area. As illustrated in Figure 4-8, it was observed that the number of repeat units per graft was a linear function of monomer feed concentration. The polymerization reaction time was 120 minutes. Polymer grafts with as many as 125 repeat units per chain were grafted with 15% monomer concentration in the feed. This indicates that the membrane has a potential for high throughput production of MABs. However, it should be noted here that significant membrane swelling and cracking was observed for a feed concentration of 20% monomer.

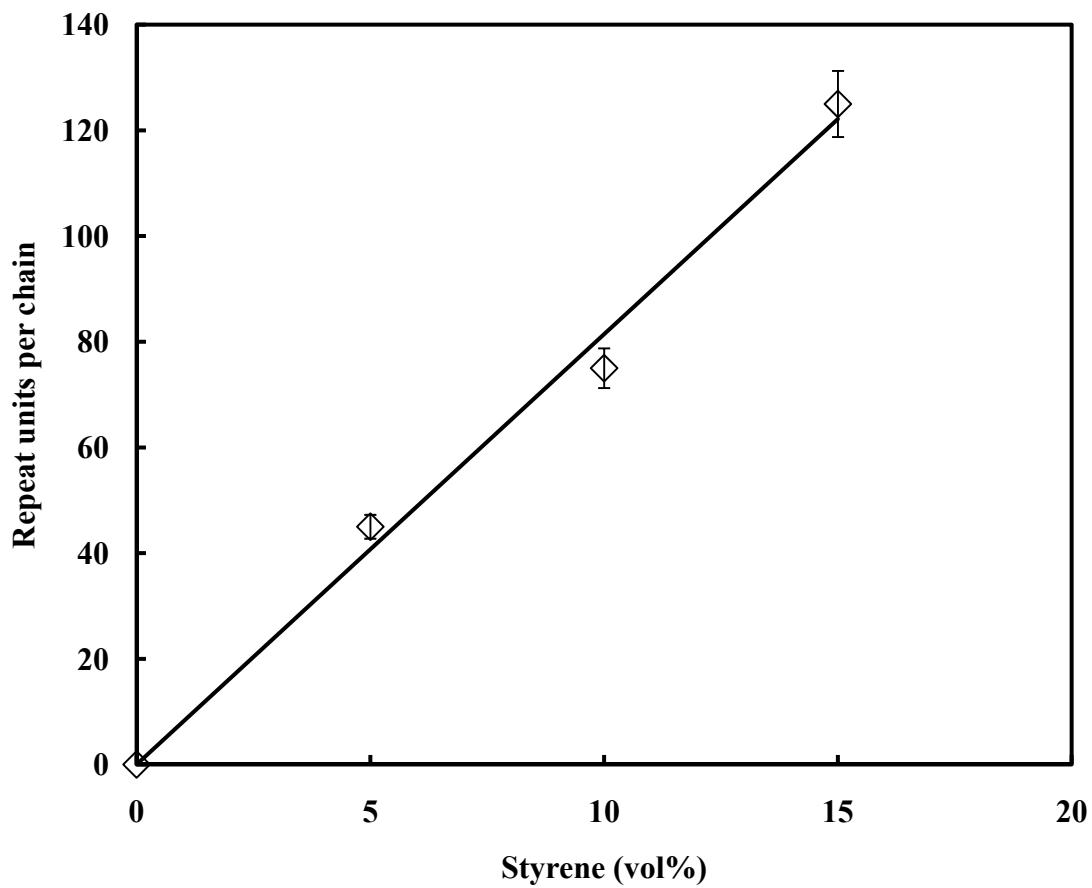


Figure 4-8. Influence of monomer feed concentration on graft length. Polymerization reaction time was 120 minutes.

4.6.3 Influence of initiator contact time

4.6.3.1 Monomer reacted

The amount of styrene retained was measured and plotted for different initiator reaction times. Monomer feed concentrations were kept constant at 5 vol% and the polymerization reaction time was 90 minutes. It can be seen from Figure 4-9 that the grafting level increased sharply with increase in initiator reaction time from 45 to 135 minutes. This is because with increase in sulfonation reaction time, more active sites are available for polymerization. After approximately 135 minutes, however, there is no significant increase in the percentage of styrene retained. This is because number of initiator sites reached a maximum, and the polymerization rate reached a corresponding peak. Similar observations were reported with respect to graft length and IEC where both the parameters plateau after approximately 135 minutes of initiator reaction time. This will be discussed in subsequent paragraphs.

4.6.3.2 Graft length

It can be observed from the Figure 4-10 that graft length in terms of number of repeat units per chain initially dropped significantly and was approximately constant after 135 minutes of initiator reaction time. This indicates that at low initiator contact time relatively long polymer chains are formed as compared to high initiator contact time. This was most likely due to crowding effects due higher initiator surface density where all active sites are not accessible at higher contact time. This also indicated that polymer growth was constant above a critical initiator surface density. This was confirmed by normalizing the data shown in Figure 4-9 where there was no significant change in amount of styrene retained after 135 minutes of initiator contact time. It should be noted that the polymerization reaction time was kept constant at 120 minutes.

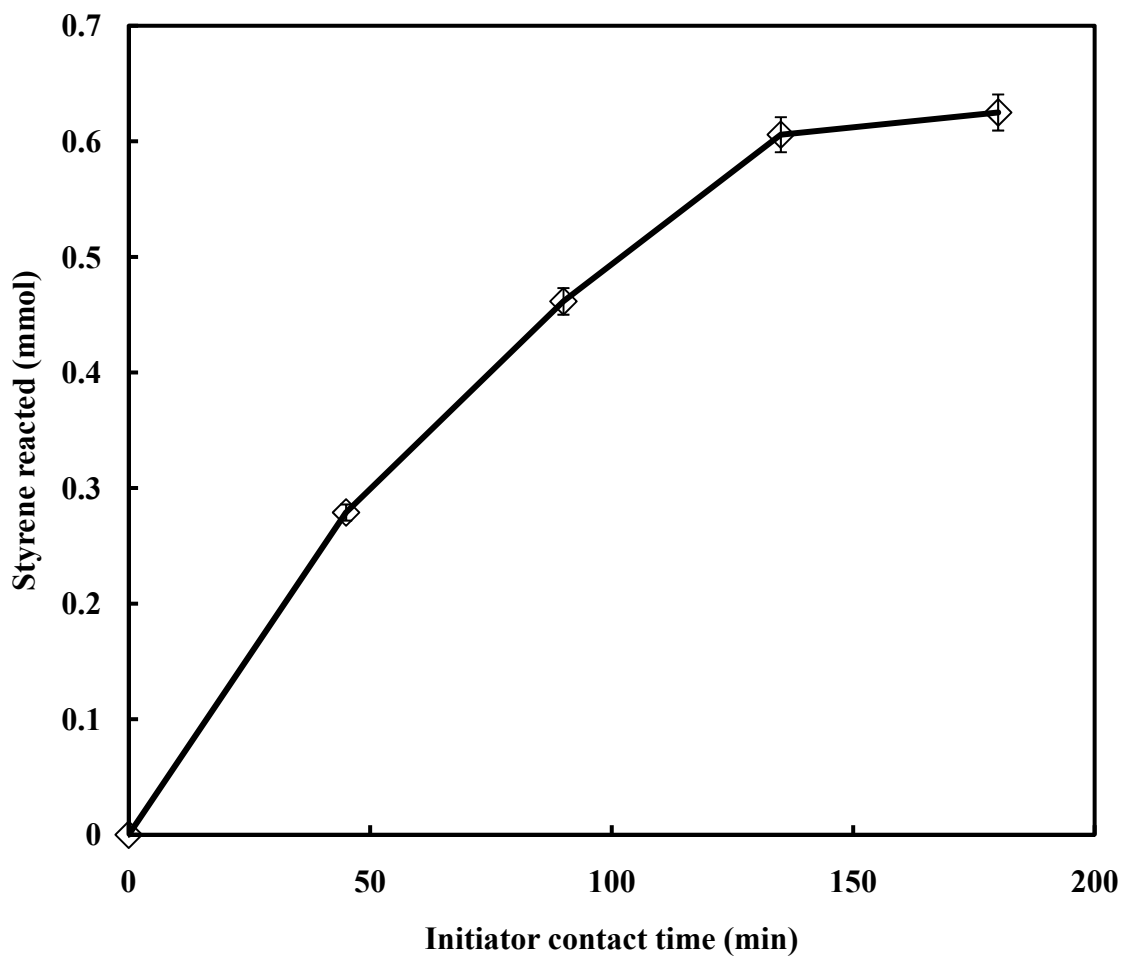


Figure 4-9. Effect of initiator reaction time on amount of styrene reacted.

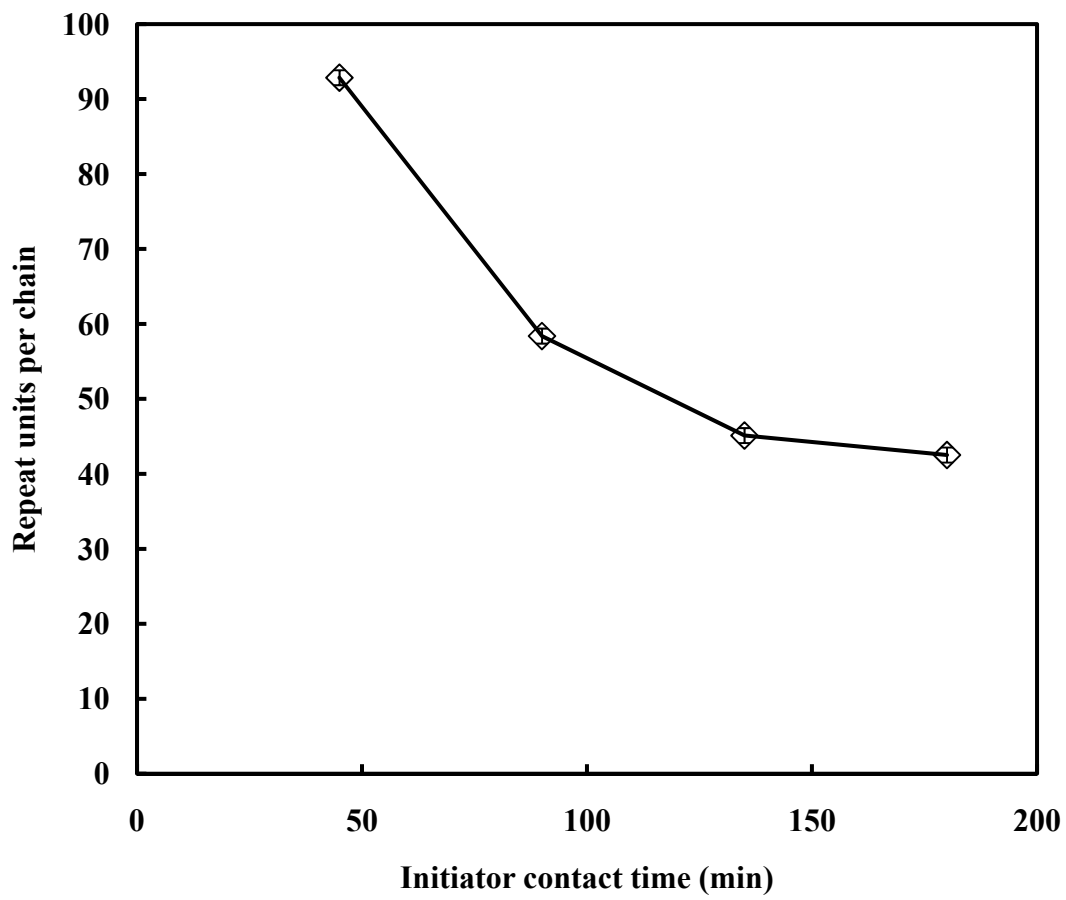


Figure 4-10. Effect of initiator reaction time on graft length.

4.6.3.3 Ion-exchange capacity

The membrane was first sulfonated at different initiator contact times. For each contact time the membrane was polymerized to form polystyrene grafts. After polymerization the membrane was again sulfonated prior to measuring the IEC of the grafted membrane. Figure 4-11 shows the effect of initiator contact time on IEC (meq/g) of the grafted membrane. The polymerization reaction time was 120 minutes for all three monomer concentrations. It can be seen that the IEC value increased with increasing initiator contact time for all three monomer concentrations. For lower initiator contact time (50 and 100 minutes) the IEC increased linearly with increased monomer concentration. After 135 minutes of initiator reaction time the IEC approached a maximum where the initiator sites were saturated and no further change in IEC was observed. Thus, at lower initiator reaction times fewer grafts were formed and IEC was lower. At higher initiator contact times the number of initiator sites available for grafting was higher, more grafts were formed and the IEC was higher. The IEC value was highest (4.9 meq/g) for 15% monomer concentration and 135 minutes of initiator reaction time. This corresponds to more than 350 times greater ion-exchange capacity than raw membrane and approximately 18 times greater than sulfonated membrane.

IEC is an indicator of dynamic and equilibrium binding capacity. For membranes, dynamic and equilibrium binding capacities are essentially the same because of the dominance of convective mass transfer and the elimination of diffusional transport limitations. Equilibrium binding capacity is expressed as the millimoles of styrene per ml of membrane. Dynamic binding capacity is expressed as millimoles of sodium ions bound to sulfonic acid groups on polystyrene grafts per ml of membrane while permeating 0.1N NaOH under defined conditions (flow rate, sulfonation and polymerization reaction time).

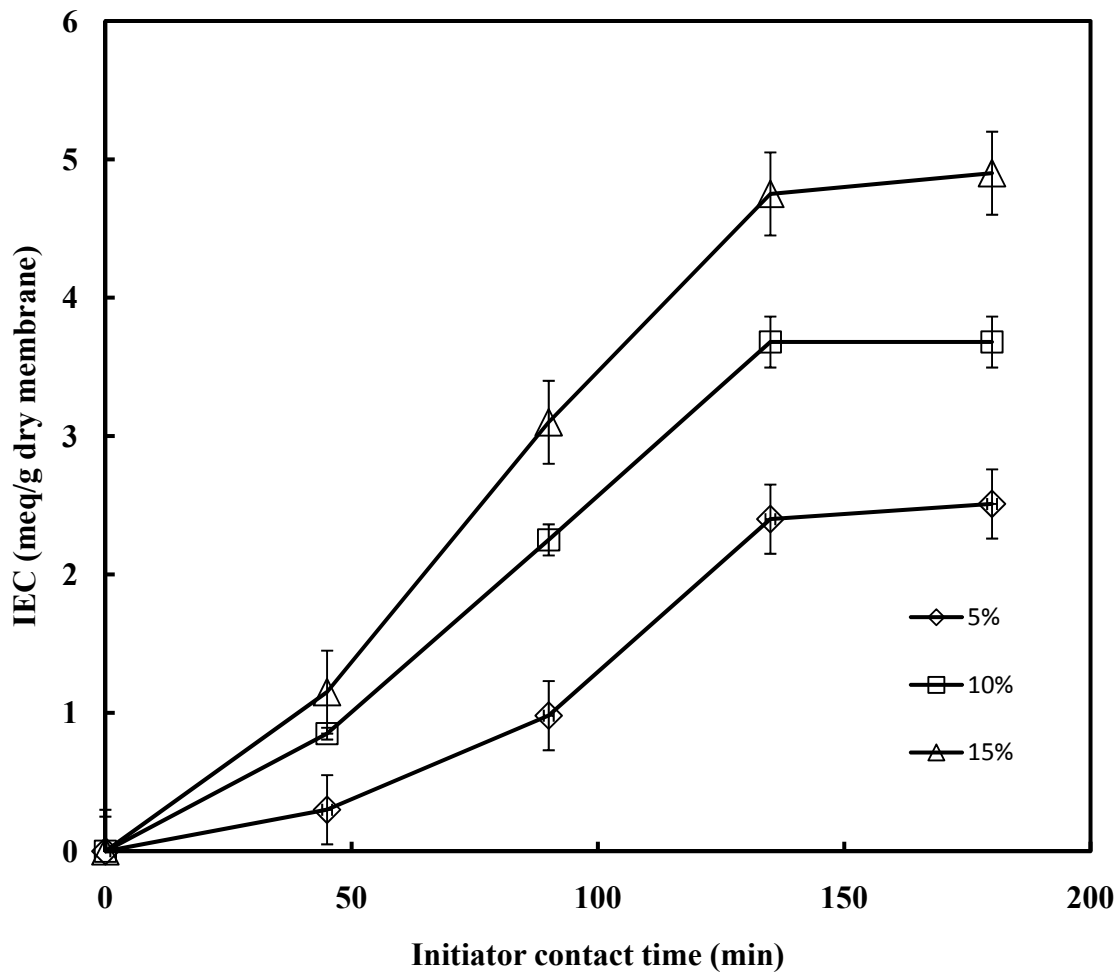


Figure 4-11. Effect of initiator reaction time and monomer feed concentration on IEC.

Functionalized membrane has a dynamic binding capacity of 5.36 mmol/ml at 135 minutes of initiator contact time, 120 minutes of polymerization reaction time and 15% monomer feed concentration. This represents roughly 90% of equilibrium binding capacity (5.94 mmol/ml). This indicates that the functionalized membrane has high dynamic and equilibrium binding capacity and should indicate similar increased capacity for purification of MAbs.

4.6.4 Summary of results from polymer growth experiments

Ion-exchange capacity and average graft length have been studied as a function of reaction parameters, initiator contact time and monomer concentration. The experimental results have been compared to show the effect of the reaction parameters (initiator reaction time and monomer concentration) on ion-exchange capacity and graft length. The polymerization reaction time was fixed at 120 minutes. It should be noted that while one reaction parameter is changed the other is kept constant and vice versa. The results from these experiments will help in better understanding the control of each of these reaction parameters. These results will be used in future for specific applications like absorption of MAbs.

4.6.4.1 Ion-exchange capacity

From the results it was observed that IEC increased approximately linearly with initiator contact times (less or equal to 135 minutes) and change in monomer feed concentration from 5 to 15%. The IEC stayed constant for initiator contact time greater than 135 minutes but it still showed linear dependency for change in monomer feed concentration. This indicated that both the reaction parameters have significant influence on IEC at lower initiator contact times. However, at higher initiator contact times, change in monomer feed concentration dominated and had a more profound effect on IEC.

4.6.4.2 Graft length

It was observed that the graft length is inversely proportional to initiator contact time (less or equal to 135 minutes) and directly proportional to monomer feed concentration. However, the graft length was nearly constant after 135 minutes of initiator contact time. Therefore, there are fewer degrees of freedom to control graft length at higher packing density. Graft length was impacted by both monomer feed concentration and initiator contact time at lower surface density.

CHAPTER 5

CONCLUSIONS

A novel polymeric, functionalized membrane has been created by cationic polymerization of styrene and substituted styrene monomers. Homopolymer and block copolymer brushes have been grafted in the pores of microfiltration PES membrane. The quantitative information from the analytical experiments and material balances showed that the material has a very high ion-exchange capacity of (4.9 meq/g) with roughly 125 repeat units per chain. This represents roughly 92% of theoretical maximum (5.3 meq/g) ion-exchange capacity of an ion-exchange resin. This indicates high dynamic and equilibrium binding capacity of the functionalized membrane. Synthesis of homopolymer and block copolymer brushes has been confirmed by UV-visible spectroscopy and gas chromatography analysis of the feed and permeate solutions. Permeability studies at each step were performed. The results revealed that there is an order of magnitude decrease in pure water permeability from raw to sulfonated to styrene grafted and finally CMS grafted membrane. This result further confirmed the presence of grafted polymer in the membrane.

Kinetics of reaction of each monomer during formation of homopolymer brush were studied. Pseudo-first-order kinetic expression correlated well with the experimental data for each monomer reacted. It was observed that CMS was the least reactive and styrene and ES showed similar reactivity during formation of homopolymer. CMS reacted approximately 25% slower as compared to styrene and ES. The low reactivity of CMS is due to the presence of a strong electron-withdrawing chloromethyl pendent group. Ethoxy moiety in the ES monomer has an electron-donor substituent which makes it more reactive relative to CMS. Similar observations were reported during formation of block copolymers poly(styrene-co-CMS) and poly(styrene-co-

ES). CMS reacted approximately 22% slower than ES after polymerization with styrene. ES and CMS showed low reactivity during formation of block copolymer as opposed to during formation of homopolymer. This may be due to diffusion barrier by polystyrene grafts already present in the pores of membrane.

Finally, controlled polymer growth of styrene monomer was studied to understand the process and control of the polymerization reactions. This was done by studying the effects of monomer concentration and initiator reaction time on polymer growth aspects like kinetics, amount of styrene reacted, IEC, and graft length. At lower initiator surface density, graft length and IEC were impacted by both monomer feed concentration and initiator contact time. However, for higher initiator surface density the monomer feed concentration parameter dominates. The results from polymer growth experiments can be utilized to determine particular initiator contact time and monomer concentration for the desired binding capacity between ligand and antibody. Additionally, the results can be used to generate customized structures for a range of monomer concentrations and reaction times.

CHAPTER 6

FUTURE WORK AND SCOPE

Functionalized membranes formed in this research show a great deal of promise for large scale purification of monoclonal antibodies. Block copolymers formed in this work will have applications to mimic the dipeptide structure of phenylalanine/tyrosine in protein A ligand which is crucial for interaction with IgG. This will further result in understanding formation of synthetic affinity ligand membrane adsorbers for protein and antibody separation.

Future research efforts will focus on understanding polymer growth aspects for ES and CMS. A mathematical model for polymer growth, validated with the experimental data, would further help in understanding the reaction mechanism. Qualitative evidence of graft characterization will be confirmed by FTIR and NMR. Amino and hydroxyl groups will be introduced to mimic the phenylalanine/tyrosine dipeptide structure. This will be done by reacting chloromethyl group with glycine and hydrolysis of the ES ethoxy group.

Functionalized membranes will be further tested for antibody adsorption. This includes determination of antibody (IgG) binding capacity and competitive sorption in the presence of bovine serum albumin (BSA). Finally, membrane pore size distribution will be determined based on rejection of solute molecules. Molecular weight distribution of feed and permeate solutions will be determined by high performance liquid chromatography and size exclusion chromatography. The average pore size distribution can be calculated based on distribution of solute particles rejected.

REFERENCES

1. Hubbuch, J.; Linden, T.; Knieps, E.; Thommes, J.; Kula, M., "Dynamics of protein uptake within the adsorbent particle during packed bed chromatography," *Biotechnology and Bioengineering* 80 (2002) 359-368.
2. Wierling, P.S.; Bogumil, R.; Knieps-Grunhagen, E.; Hubbuch, J., "High-throughput screening of packed-bed chromatography coupled with SELDI-TOF MS analysis: Monoclonal antibodies versus host cell protein," *Biotechnology and Bioengineering* 80 (2002) 440-450.
3. Hage, D.S., "Affinity chromatography: A review of clinical applications," *Clinical Chemistry* 45 (1999) 593-615.
4. Ghosh, R., "Protein separation using membrane chromatography: opportunities and challenges," *Journal of Chromatography A* 952 (2002) 13-27.
5. Lutkemeyer, D.; Bretschneider, M.; Buntmeyer, H.; Lehmann, J., "Membrane chromatography for rapid purification of recombinant antithrombin III and monoclonal antibodies from cell culture supernatant," *Journal of Chromatography* 639 (1993) 57-66.
6. Champluvier, B.; Kula, M.R., "Dye-ligand membranes as selective adsorbents for rapid purification of enzymes: A case study," *Biotechnology and Bioengineering* 40 (1991) 33-40.
7. Kiyohara, S.; Kim, M.; Toida, Y.; Kyoichi, S.; Kazuyuki S., "Selection of a precursor monomer for the introduction of affinity ligands onto a porous membrane by radiation-induced graft polymerization," *Journal of Chromatography A* 758 (1997) 209-215.
8. Champluvier, B.; Kula, M.R., "Microfiltration membranes as pseudo-affinity adsorbents: modification and comparison with gel beads," *Journal of Chromatography A* 539 (1991) 315-325.
9. Briefs, K.G.; Kula, M.R., "Fast protein chromatography on analytical and preparative scale using modified microporous membranes," *Chemical Engineering Science* 47 (1992) 141-149.
10. Tennikova, T.B.; Svec, F., "High-performance membrane chromatography: highly efficient separation method for proteins in ion-exchange, hydrophobic interaction and reversed-phase modes," *Journal of Chromatography A* 646 (1993) 279-288.
11. Suen, S.Y.; Etzel, M.R., "A mathematical analysis of affinity membrane bioseparations," *Chemical Engineering Science* 47 (1992) 1355-1364.

12. Lightfoot, E.N.; Coffman, J.L.; Lode, F.; Yuan, Q.S.; Perkins, T.W.; Root, T.W., "Refining the description of protein chromatography," *Journal of Chromatography A* 760 (1997) 139-149.
13. Shah, T.N.; Ritchie, S.M.C., "Esterification catalysis using functionalized membranes," *Journal of Applied Catalysis A* 296 (2005) 12-20.
14. Yang, L.; Biswas, M.E.; Chen, P., "Study of binding between protein A and immunoglobulin G using a surface tension probe," *Biophysical Journal* 84 (2003) 509-522.
15. Yang, L.; Biswas, M.E.; Chen, P., "The interaction of Protein A and the Fc fragment of rabbit immunoglobulin G as probed by complement-fixation and nuclear-magnetic-resonance studies," *Biochemistry Journal* 167 (1997) 661-668.
16. <http://en.wikipedia.org/wiki/Monoclonalantibodies>.
17. Hamada, H.; Takashi, T., "Determination of membrane antigens by a covalent crosslinking method with monoclonal antibodies," *Analytical Biochemistry* 160 (1987) 483-488.
18. Chaudhuri, T.R.; Zinn, K.R.; Morris J.S.; McDonald, G.A.; Llorens, A.S.; Chaudhuri, T.K., "Human monoclonal antibody developed against ovarian cancer cell surface antigen," *Cancer* 73 (1994) 1098-1104.
19. John Mascola, M.D., "Combination HIV-IG/Monoclonal antibody dose neutralizes AIDS virus," *Fourth Conference on Retroviruses and Opportunistic Infections* (1997) Washington, D.C.
20. Dirk, R.J.K.; Yves F.C.V., "Monoclonal antibodies in renal transplantation: old and new," *Nephrology Dialysis Transplantation* 19 (2004) 297-300.
21. Djuro, J.; Yow-Pin, L., "Analytical and preparative methods for purification of antibodies," *Food Technology and Biotechnology* 39 (3) (2001) 215-226.
22. Przybycien, T.M.; Pujar, N.S.; Steele, L.M., "Alternative bioseparation operations: life beyond packed-bed chromatography," *Current Opinion in Biotechnology* 15 (2004) 469-478.
23. Schure, M.R.; Maier, R.S.; Kroll, D.M.; Davis, H.T., "Simulation of packed-bed chromatography utilizing high-resolution flow fields: Comparison with models," *Biotechnology and Bioengineering* 80 (2002) 359-368.
24. Huse, K.; Bohme, H.J.; Scholz, G.H., "Purification of antibodies by affinity chromatography," *Journal of Biochemical and Biophysical Methods* 51 (2002) 217-231.

25. Van Reis, R.; Zydney, A., "Membrane separations in biotechnology," *Current Opinion in Biotechnology* 12 (2001) 208-211.
26. Hanfa, Z.; Quanzhou, L.; Dongmei, Z., "Affinity membrane chromatography for the analysis and purification of proteins," *Journal of Biochemical and Biophysical Methods* 49 (2001) 199-240.
27. http://en.wikipedia.org/wiki/Affinity_chromatography.
28. Gustavsson, P.; Mosbach, K.; Nilsson, K.; Larsson, P., "Superporous agarose as an affinity chromatography support," *Journal of Chromatography A* 776 (1997) 197-203.
29. Newcombe, A.R.; Cresswell, C.; Davies, S.; Watson, K.; Harris, G.; O'Donovan, K.; Francis, R., "Optimised affinity purification of polyclonal antibodies from hyper immunized ovine serum using a synthetic Protein A adsorbent, MAbsorbent A2P," *Journal of Chromatography B* 814 (2005) 209-215.
30. Teng, S.F.; Sproule, K.; Husain, A.; Lowe, C.R., "Affinity chromatography on immobilized "biomimetic" ligands: synthesis, immobilization, and chromatographic assessment of an immunoglobulin G-binding ligand," *Journal of Chromatography B* 740 (2000) 1-15.
31. Fassina, G.; Menotti R.; Palombo, A.V.; Marino, M., "Novel ligands for the affinity-chromatographic purification of antibodies," *Journal of Biochemical and Biophysical Methods* 49 (2001) 481-490.
32. Kabir, S., "Immunoglobulin purification by affinity chromatography using protein A mimetic ligands prepared by combinatorial chemical synthesis," *Immunological Investigations* 31 (2002) 263-278.
33. Torres B.V.; Smith, D.F., "Purification of Forssman and human blood group A glycolipids by affinity chromatography on immobilized helix promatia lectin," *Analytical Biochemistry* 170 (2004) 209-219.
34. Aubry, A., "Applications of affinity chromatography to the study of drug-melanin binding interactions," *Journal of Chromatography B* 768 (2002) 67-74.
35. Fassina, G.; Verdoliva, A.; Palombo, G.; Ruvo, M.; Cassani, G., "Immunoglobulin specificity of TG 19318: a novel synthetic ligand for antibody affinity purification," *Journal of Molecular Recognition* 11 (1998) 128-133.

36. Houghten, R.A.; Pinilla, C.; Blondelle, S.E.; Appel, J.R.; Dooley, C.T.; Cuero, J.H., "Generation and use of synthetic peptide combinatorial libraries for basic research and discovery," *Nature* 354 (1991) 84-86.
37. Lam, K.S.; Salmon, S.E.; Hersh, E.M.; Hruby, V.J.; Kazmiersky, W.M.; Knapp, R.J., "A new type of synthetic peptide library for identifying ligand-binding activity," *Nature* 354 (1991) 82-84.
38. Evensen, E.; Joseph-McCarthy, D.; Weiss, G.A.; Schreiber S.L.; Karplus, M., "Ligand design by a combinatorial approach based on modeling and experiment: application to HLA-DR4," *Journal of Computer Aided Molecular Design* 7 (2007) 395-418.
39. Fuglistaller, P., "Comparison of immunoglobulin binding capacities and ligand leakage using eight different protein A affinity matrices," *Journal of Immunological Methods* 124 (1989) 121-127.
40. Zatta, P.F., "A new bioluminescent assay for studies of protein G and protein A binding to IgG and IgM," *Journal of Biochemical and Biophysical Methods* 32 (1996) 33-43.
41. Scott, M.A.; Davis, J.M.; Schwartz, K.A., "Staphylococcal protein A binding to canine IgG and IgM," *Veterinary Immunology and Immunopathology* 59 (1997) 205-212.
42. Nevens, J.R.; Mallia, A.K.; Wendt M.W.; Smith, P.K., "Affinity chromatographic purification of IgM antibodies utilizing immobilized mannan binding protein," *Journal of Chromatography A* 597 (1992) 247-253.
43. Waldam, R.H.; Mach J.P.; Stella M.M.; Rowe D.S., "Secretory IgA in human serum" *Journal of Immunological Methods* 105 (1970) 43-47.
44. Khayam-Bashi, H.; Blanken R.M.; Schwartz C.L., "Chromatographic separation and purification of secretory IgA from human milk," *Preparative Biochemistry and Biotechnology* 7 (1977) 225-229.
45. Litman, G.W.; Good R.A., "Rapid purification of IgA from normal human serum," *Biochimica et Biophysica Acta (BBA)- Protein Structure* 263 (1972) 89-93.
46. Phillips, T.M.; More, N.S.; Queen, W.D.; Thompson, A.M., "Isolation and quantitation of serum IgE levels by high-performance immunoaffinity chromatography," *Journal of Chromatography* 327 (1985) 205-211.
47. Lehrer, S.B., "Isolation of IgE from normal mouse serum," *Immunology* 36 (1979) 103-109.

48. Schenck, H.; Unger, R.H., "Ligand leakage from immunoaffinity column," *Scandinavian Journal of Clinical and Laboratory Investigation* 43 (1983) 527-531.
49. Ikeyama, S.; Nakagawa, S.; Arakawa, M.; Sugino, H.; Kakinuma, A., "Purification and characterization of IgE produced by human myeloma cell line, U266," *Molecular Immunology* 23 (1986) 159-167.
50. Peng, Z.; Becker, A.B.; Simons, F.E., "Binding properties of protein A and protein G for human IgE," *International Archives of Allergy and Immunology* 104 (1994) 204-206.
51. Kronvall, G.; Seal, U.S.; Svensson, S.; Williams Jr., R.C., "Phylogenetic aspects of staphylococcal Protein A-reactive serum globulins in birds and mammals," *Microbiology and Immunology* 82 (1974) 12-18.
52. Taylor, A.I.; Bevil, R.L.; Sutton, B.J.; Calvert, R.A., "A monomeric chicken IgY receptor binds IgY with 2:1 stoichiometry," *The Journal of Biological Chemistry* 284 (36) (2009) 168-165.
53. Lowe, C.R.; Burton, S.J.; Burton, N.P.; Alderton, W.K.; Pitts, J.M.; Thomas, J.A., "Designer dyes: 'Biomimetic' ligands for the purification of pharmaceutical proteins by affinity chromatography," *Trends in Biotechnology* 10 (1992) 442-448.
54. Lowe, C.R.; Burton, S.J.; Burton, N.; Stewart, D.J.; Purvis, D.R.; Pitfield, I.; Eapen, S., "New developments in affinity chromatography," *Journal of Molecular Recognition* 3 (1990) 117-122.
55. Orengo, C.A.; Michie, A.D.; Jones, S.; Jones, D.T.; Swindells, M.B.; Thornton, J.M., "CATH- a hierarchic classification of protein domain structures," *Structure* 5 (1997) 1093.
56. Li, R.X.; Dowd, V.; Stewart, D.J.; Burton, S.J.; Lowe, C.R., "Design synthesis and application of a protein A mimetic," *Nature Biotechnology* 16 (1998) 190-195.
57. Teng, S.F.; Sproule, K.; Hussain, A.; Lowe, C.R., "A strategy for the generation of biomimetic ligands for affinity chromatography. Combinatorial synthesis and biological evaluation of an IgG binding ligand," *Journal of Molecular Recognition* 12 (1999) 67-75.
58. Fassina, G.; Verdoliva, A.; Odierna, M.R.; Ruvo, M.; Cassani, G., "Protein A mimetic peptide ligand for affinity purification of antibodies," *Journal of Molecular Recognition* 9 (1996) 564-569.
59. Palombo, G.; Rossi, M.; Cassani, G.; Fassina, G., "Affinity purification of mouse monoclonal IgE using a protein A mimetic ligand (TG19318) immobilized on solid supports," *Journal of Molecular Recognition* 11 (1999) 247-249.

60. Fassina, G.; Verdoliva, A.; Palombo, G., "Affinity purification of immunoglobulin M using a novel synthetic ligand," *Journal of Chromatography B* 715 (1998) 137-145.
61. Li, R.; Dowd, V.; Steward, D.J.; Burton, S.J.; Lowe, C.R., "Design, synthesis, and application of a protein A mimetic," *Nature Biotechnology* 16 (1998) 190-195.
62. Buday, Z.; Linden, J.C.; Karim, M.N., "Improved acetone-butanol fermentation analysis using subambient HPLC column temperature," *Enzyme and Microbial Technology* 12 (1990) 24-27.
63. Schoenmakers, P.J.; Uunk, L.G., "Effect of column pressure drop in packed-columns supercritical-fluid chromatography," *Chromatographia* 1 (1987) 51-57.
64. Schisla, D.K.; Carr, P.W.; Cussler, E.L., "Hollow fiber array affinity chromatography," *Biotechnology* 11 (1995) 651-658.
65. Knudsen, H.L.; Fahrner, R.L.; Xu, Y.; Norling, L.A.; Blank, G.S., "Membrane ion-exchange chromatography for process-scale antibody purification," *Journal of Chromatography A* 907 (2001) 145-154.
66. Wang, L.; Ghosh, R., "Purification of humanized monoclonal antibody by hydrophobic interaction membrane chromatography," *Journal of Chromatography A* 1107 (2006) 104-109.
67. Ritchie, S.M.C.; Bhattacharya, D., Polymeric ligand-based functionalized materials and membranes for ion-exchange, in: A.K. Sengupta, Y. Marcus (Eds.), *Ion Exchange and Solvent Extraction*, Marcel Dekker Inc., 14 (2000) 81-118.
68. Briefs, K.G.; Kula, M.R., "Fast protein chromatography on analytical and preparative scale using modified microporous membranes," *Chemical Engineering Science* 47 (1992) 141-149.
69. McGregor, W.C.; Szesko, D.P.; Mandaro, R.M.; Rai, V.R., "High performance isolation of a recombinant protein on composite ion-exchange media," *Bio/Technology* 4 (1986) 526-527.
70. Charcosset, C.; Su, Z.; Karoor, S.; Daun, G.; Colton, C.K., "Protein A immunoaffinity hollow fiber membranes for immunoglobulin purification: experimental characterization," *Biotechnology Bioengineering* 48 (1995) 415-427.
71. Krause, S.; Kroner, K.H.; Deckwer, W.D., "Comparison of affinity membranes and conventional affinity matrices with regard to protein purification," *Biotechnology Techniques* 5 (1991) 199-204.

72. Luksa, J.; Menart, V.; Milicic, S.; Kus, B.; Gaberc-Porekar, V.; Josic, D., "Purification of human tumor necrosis factor by membrane chromatography," *Journal of Chromatography A* 661 (1994) 161-168.
73. Cristiana, B., "Membrane adsorbers as purification tools for monoclonal antibody purification," *Journal of Chromatography B* 848 (2007) 19-27.
74. Tennikova, T.B.; Bleha, M.; Svec, F.; Almazova, T.V.; Belenkii, B.G., "High performance membrane chromatography of proteins, a novel method of protein separation," *Journal of Chromatography A* 555 (1991) 97-107.
75. Tennikova, M.B.; Gazdina, N.V.; Tennikova, T.B.; Svec, F., "Effect of porous structure of macroporous polymer supports on resolution in high-performance membrane chromatography of proteins," *Journal of Chromatography A* 798 (1998) 55-64.
76. Sarfert, F.T.; Etzel, M.R., "Mass transfer limitations in protein separations using ion-exchange membranes," *Journal of Chromatography A* 764 (1997) 3-20.
77. Yang, H.; Viera, C.; Fisher, J.; Etzel, M.R., "Purification of a large protein using ion-exchange membranes," *Industrial Engineering and Chemistry Research* 41 (2002) 1597-1602.
78. Kiyohara, S.; Sasaki, M.; Saito, K., "Amino acid addition to epoxy-group-containing polymer chain grafted onto a porous membrane," *Journal of Membrane Science* 109 (1996) 87-92.
79. Kim, M.; Saito, K.; Furusaki, S., "Adsorption and elution of bovine γ -globulin using an affinity membrane containing hydrophobic amino acids as ligands," *Journal of Chromatography* 585 (1991) 45-51.
80. Malakian, A.; Golebiowska, M.; Bellefeuille, J., "Purification of monoclonal and polyclonal IgG with affinity membrane matrix coupled with proteins A and G," *American Laboratory* 25 (1993) 40P-40V.
81. Charcosset, C.; Su, Z.; Karoor, S.; Daun, G.; Colton, C.K., "Protein A immunoaffinity hollow fiber membranes for immunoglobulin purification: experimental characterization," *Biotechnology and Bioengineering* 48 (1995) 415-427.
82. Bueno, S.M.A.; Haupt, K.; Vijayalakshmi, M.A., "In vitro removal of human IgG by pseudobiospecific affinity membrane filtration on a large scale," *International Journal of Artificial Organs* 18 (7) (1995) 392-398.

83. Woker, R.; Champluvier, B.; Kula, M.R., "Purification of S-oxynitrilase from Sorghum bicolor by immobilized metal ion affinity chromatography on different carrier materials," *Journal of Chromatography B* 584 (1992) 85-92.
84. Suen, S.; Etzel, M.R., "A mathematical analysis of affinity membrane bioseparations," *Chemical Engineering Science* 47 (1992) 1355-1364.
85. Ritchie, S.M.C., "Guest viewpoint: Recent advancements in functionalized polymeric membranes," *Membrane Quarterly* 18 (2003) 5-9.
86. Ritchie, S.M.C., "Polymer grafted membranes," Chapter 15 of *New Insights into Membrane Science and Technology: Polymeric and Biofunctional Membranes*, ed. D. Bhattacharyya and D. A. Butterfield, Elsevier, 2003.
87. Osada, Y.; Honda, K.; Ohta, M., "Control of water permeability by mechanochemical contraction of poly(methacrylic acid)-grafted membranes," *Journal of Membrane Science* 27 (1986) 327-338.
88. Milner, S.T., "Polymer brushes," *Science* 22 (1991) 905-914.
89. Halperin, A.; Tirrell, M.; Lodge T.P., "Tethered chains in polymer microstructures," *Advances in Polymer Science* 100 (1992) 31-71.
90. Szlefer, I.; Carignano M.A., "Tethered polymer layers," *Advances in Chemical Physics* 94 (1996) 165-260.
91. Soga K.; Zukermann M.J.; Guo, H., "Binary polymer brush in a solvent," *Macromolecules* 29 (1996) 1998-2005.
92. Mansky, P.; Liu, Y.; Huang, E.; Russell, T.P.; Hawker, C., "Controlling polymer-surface interactions with random copolymer brushes," *Science* 275 (1997) 1458-1460.
93. Zhao, B.; Brittain, W.J., "Polymer brushes: surface-immobilized macromolecules," *Progress in Polymer Science* 25 (2000) 677-710.
94. Zhao, B.; Brittain, W.J., "Synthesis of tethered polystyrene-block-poly(methyl methacrylate) monolayer on a silicate substrate by sequential carbocationic polymerization and atom transfer radical polymerization," *Journal of The American Chemical Society* 121 (1999) 3557-3558.
95. Faust, R.; Kennedy, J.P., "Living carbocationic polymerization of styrene," *Polymer Bulletin* 19 (1988) 21-28.

96. http://en.wikipedia.org/wiki/Anionic_addition_polymerization.
97. Hirao, A.; Nagahama, T.; Ishizone, S., "Synthesis of polymers with carboxy end groups by reaction of polystyryl anions with 4-bromo-1,1,1-trimethoxybutane," *Macromolecules* 26 (1993) 2145-2150.
98. Quirk, R.P.; Zhu, L., "Anionic synthesis of chain-end functionalized polymers using 1,1-diphenylethylene derivatives. Preparation of 4-hydroxyphenyl-terminated polystyrenes," *Macromolecular Chemistry and Physics* 190 (1989) 487-493.
99. Hayashi, M.; Nakahama, S.; Hirao, A., "Synthesis of end-functionalized polymers by means of living anionic polymerization. Reaction of living anionic polymerization with halopropyl styrene derivatives," *Macromolecules* 32 (1999) 1325-1331.
100. Szwarc, M.; Beylen, M.V., *Ionic polymerization and living polymers*. New York: Chapman, 1993.
101. Ritchie S.M.C.; Bachas, L.G.; Olin, T.; Sikdar, S.K.; Bhattacharyya, D., "Surface modification of silica- and cellulosic-based microfiltration membranes with functional polyamino acids for heavy metal sorption," *Langmuir* 15 (1999) 6346-6357.
102. Ritchie, S.M.C.; Kissick, K.E.; Bachas, L.G.; Sikdar, S.K.; Parikh, C.; Bhattacharyya, D., "Polycysteine and other polyamino acid functionalized microfiltration membranes for heavy metal capture," *Environmental Science & Technology* 35 (2001) 3252-3258.
103. Mark, H.F.; Bikales, N.M.; Overberger, C.G.; Menges, G., *Encyclopedia of polymer science and engineering*, 2nd edition, John Wiley & Sons, New York, 1985.
104. Matyjaszewski, K., *Cationic polymerizations*. New York: Dekker, 1996.
105. Ishihama, Y.; Sawamoto, M.; Higashimura, T., "Living cationic polymerization of styrene by the methanesulfonic acid/ tin tetrachloride initiating system in the presence of tetra-n-butylammonium chloride," *Polymer Bulletin* 23 (1990) 361-366.
106. Kostjuk, S.V.; Kapytsky, F.N.; Mardykin, V.P.; Gaponik, L.V.; Antipin, L.M., "Living cationic polymerization of styrene with 1-phenylethylchloride/TiCl₄/BU₂O," *Polymer Bulletin* 49 (2002) 251-256.
107. Guiver M.D.; Croteau S.; Hazlett J.D.; Kutowy, O., "Synthesis and characterization of carboxylated polysulfones," *British Polymer Journal* 23 (1990) 29-39.

108. Blanco J.F.; Nguyen, Q.T.; Schaetzel, P., "Novel hydrophilic membrane materials: sulfonated polyethersulfone Cardio," *Journal of Membrane Science* 186 (2001) 267-279.
109. Cowan, S.; Ritchie, S., "Modified polyethersulfone (PES) ultrafiltration membranes for enhanced filtration of whey proteins," *Separation Science and Technology* 42 (2007) 2405-2418.
110. Shah, T.N.; Goodwin, J.C.; Ritchie, S.M.C., "Development and characterization of a microfiltration membrane catalyst containing sulfonated polystyrene grafts," *Journal of Membrane Science* 251 (2005) 81-89.
111. Ozcan, A.; Ozcan, A.S., "Adsorption of Acid Red 57 from aqueous solutions onto surfactant-modified sepiolite," *Journal of Hazardous Materials B* 125 (2005) 252-259.
112. Zermane, F.; Bouras, O.; Baudu, M.; Basly, J-P., "Cooperative coadsorption of 4-nitrophenol and basic yellow 28 dye onto an iron organo-inorgano pillared montmorillonite clay," *Journal of Colloid and Interface Science* 350 (2010) 315-319.
113. Allcock, H.; Fitzpatrick, R., "Sulfonation of (Aryloxy)- and (Arylamino) phosphazenes: Small-molecule compounds, polymers, and surfaces," *Chemistry of Materials* 3 (1991) 1120-1132.
114. Hollman, A.M.; Scherrer, N.T.; Cammers-Goodwin, A.; Bhattacharyya, D., "Separation of dilute electrolytes in poly(amino acid) functionalized microporous membranes: model evaluation and experimental results," *Journal of Membrane Science* 239 (2004) 65-79.
115. Kamigaito, M.; Nakashima, J.; Satoh, K.; Sawamoto, M., "Controlled cationic polymerization of p-(chloromethyl)styrene: BF₃-catalyzed selective activation of a C-O terminal from alcohol," *Macromolecules* 36 (2003) 3540-3544.